

Geotechnical Engineering

Review of Some Basic Aspects

by

Dieter Stolle

Introduction

All structures that are designed and built by Civil Engineers are connected in some way to the earth. They are either supported by the geosphere or support the ground. Foundations provide the connection between man-made structures and the geosphere, with foundation engineering being concerned with soil-structure interaction. Geotechnical Engineering II introduces the background theory required in foundation engineering.

This is a three credit undergraduate course in Civil Engineering and is a extension of Geotechnical I, which focuses on stresses in the ground, as well as on settlements. The main purpose of the Civ Eng 3B03 is to introduce the principles of shear strength theory, which are required for the design and analyses of foundations of structures, including buildings, bridges, and retaining structures. Topics addressed in this course include: shear strength characteristics and failure criteria for soils; direct shear, triaxial, plane strain and field tests; earth pressure theory; bearing capacity theory; slope stability and embankment analysis. Before tackling the main themes of this course, a brief review is given of the background material.

General

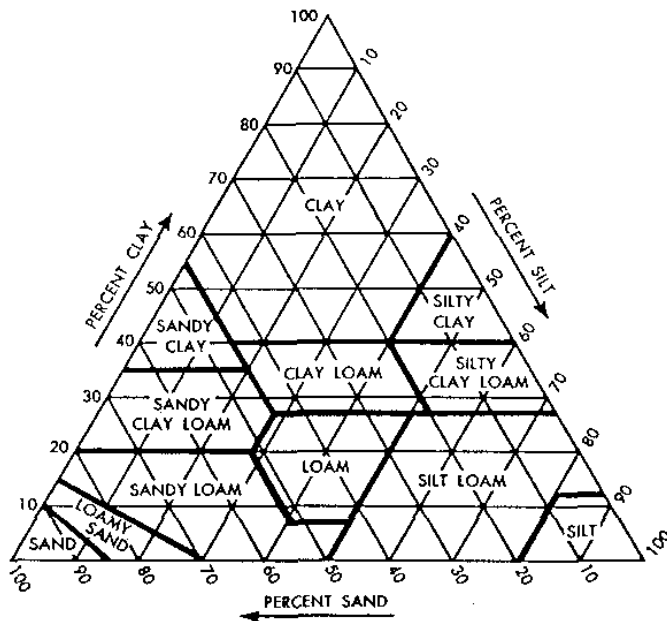
Soils are particulate materials formed by weathering of rock or by decomposition of organic matter. There are two types of weathering:

- **physical weathering** - frictional type erosion, freeze-thaw, thermal expansion, etc.
- **chemical weathering** - hydration, oxidation, reduction, etc.

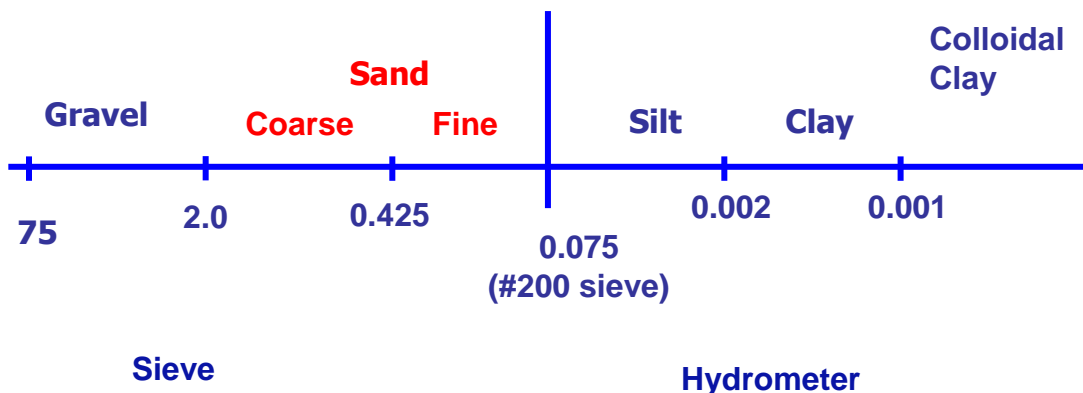
Soil properties can vary considerably, depending on the history of formation. In Southern Ontario most of our soils have been transported and deposited via glacial activity.

Soils generally consist of particles of various grain size. Most soil classification systems describe a soil according to the constituent(s), which control the material's mechanical behaviour. One simple system, for example, developed by the US Bureau of Public

Roads, considers three main groups: sand, silt and clay. Soils, which contain mostly sand and silt, are referred to as *loams*. This particular system recognizes the fact that *a soil containing more than 30% clay behaves essentially as clay*.



The American Association of State Highway and Transportation Officials (AASHTO) suggest the following:



It is important to recognize that these sizes refer to nominal diameters, obtained via some "filtering" process, which tunes in on a perceived (not true) size.

Table 1: Summary of General Soil Characteristics

Soil	Weathering Mode	Characteristics
Gravel	physical	- rock fragments - angular if only slightly worn - quartz, granite, basalt, limestone
Coarse Sand	physical	- same constituents as gravel - more rounded
Fine Sand	physical	- often more angular than coarse sand due to protective water film
Note: Coarse aggregate properties depend on particle shape, size and gradation.		
Silts	physical and chemical	- properties between those of chemical clays and non-cohesive soils
Clays	chemical	- surface forces dominate - properties dictated by surface chemistry and moisture content - effect of gradation not as important

Phase Relationships

Soil is a three-phase material: solid, liquid and gas. To describe the state of the soil, one makes use of simple mass and volumetric measures:

- water content: $w = \frac{M_w}{M_s}$
- moisture content: $m = \frac{M_w}{M} = \frac{w}{1+w}$
- void ratio: $e = \frac{V_v}{V_s}$
- relative density $D_r = \frac{e_{\max} - e}{e_{\max} - e_{\min}} \times 100$
- degree of saturation: $S = \frac{V_w}{V_v} = \frac{wG_s}{e}$
- bulk density: $\rho = \frac{M}{V} = \frac{G_s(1+w)}{1+e} \rho_w$

where M and V denote mass and volume, respectively, with the subscripts s , w and v referring to solid, water and voids, respectively. It should be noted that the voids are considered to be all of the non-solid phase; i.e. combined air and water volume.

Atterberg Limits

The consistency of a fine-grained soil at various water contents depends on its mineralogy. There are three states of interest:

- liquid limit w_l – transition from plastic to liquid state of remolded material
- plastic limit w_p – transition from semi-solid to plastic state, where material undergoes deformation at zero volume change
- shrinkage limit w_s – lowest water content at which material is still saturated; i.e., soil sample will not reduce its volume further without drying

The plastic index is defined as: $I_p = w_l - w_p$

The Atterberg limits together with information on grain size distribution are valuable for soil classification via, for example, the Unified Classification System (UCS).

Unified Classification System

The Unified Classification System, developed by Casagrande in 1940, provides the engineer with more information than that introduced in the previous section. It is based on using a prefix which indicates the dominant soil type, and a suffix which acts as a modifier. This section briefly reviews the logic associated with the labelling of a soil. It should be noted that the procedure described below has been updated in order to be more precise in the description for soil. For the updated system, the student should consult ASTM D-2487.

Decide whether fine or coarse-grained.

(a) If **coarse-grained** then > 50% is retained on the #200 sieve.

- Determine dominant size range of coarse fraction (provides prefix).

G = Gravel > 50% of coarse retained on #4 sieve

S = Sand < 50% of coarse retained on #4 sieve

- Determine soil distribution characteristics (provides suffix).

W = well-graded, < 5% fines

P = poorly-graded, < 5% fines

M = contains silt, or silt and sand, > 12% fines

C = contains clay, or sand and clay, > 12% fines

If the percent fines is between 5 and 12, then a dual classification is required; e.g. SP-SM, GW-GC, etc.

- (b) If **fine-grained** then < 50% is retained on the #200 sieve.

- Determine whether behaviour dominated by surface forces or by body forces (provides prefix).

C = clay, on or above A-line

M = silt, silt and silty clay, below A-line

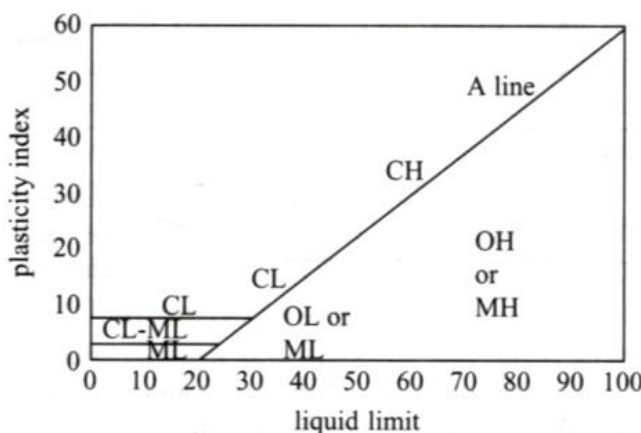
O = organic silt or organic clay

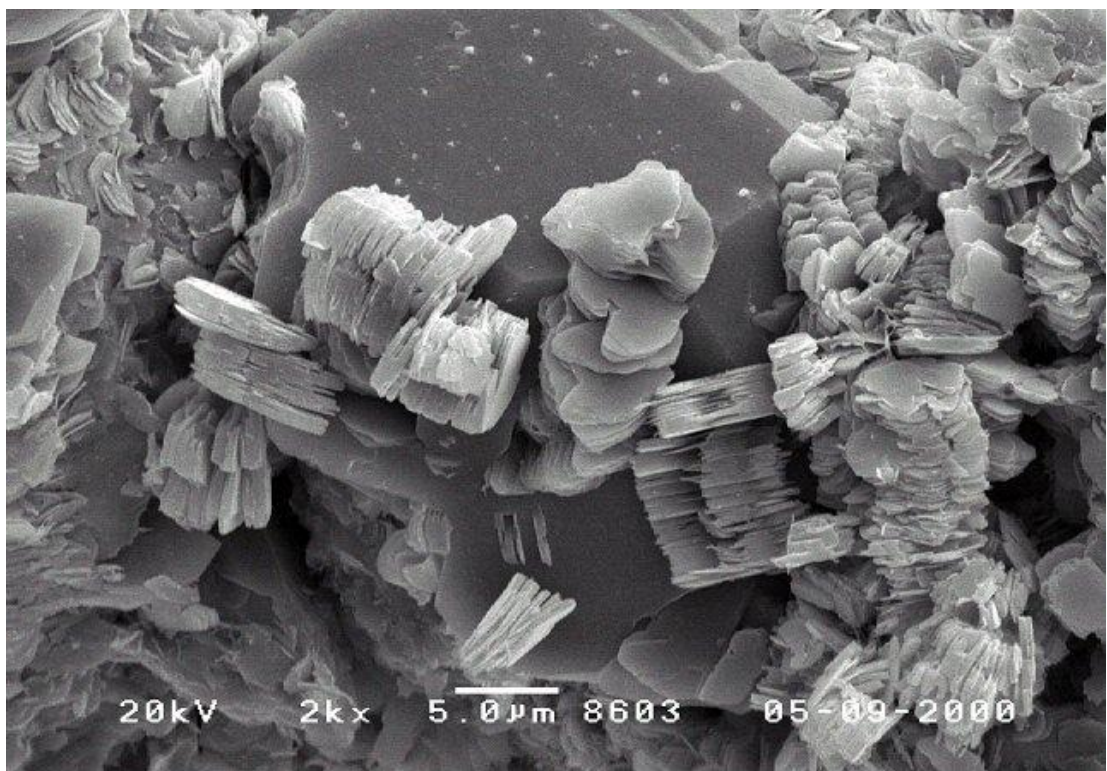
($w_L\text{-oven} < 0.75 w_L\text{-air}$)

- Determine level of plasticity (provides suffix).

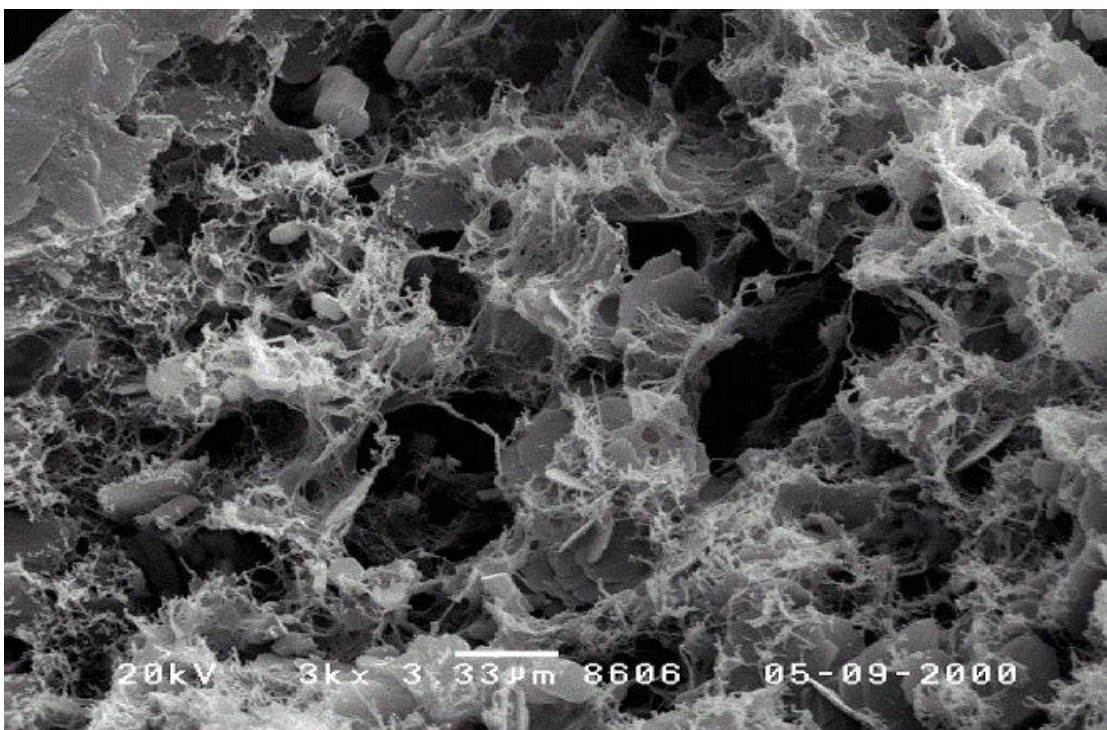
L = low plasticity, $w_L < 50$

H = high plasticity, $w_L > 50$

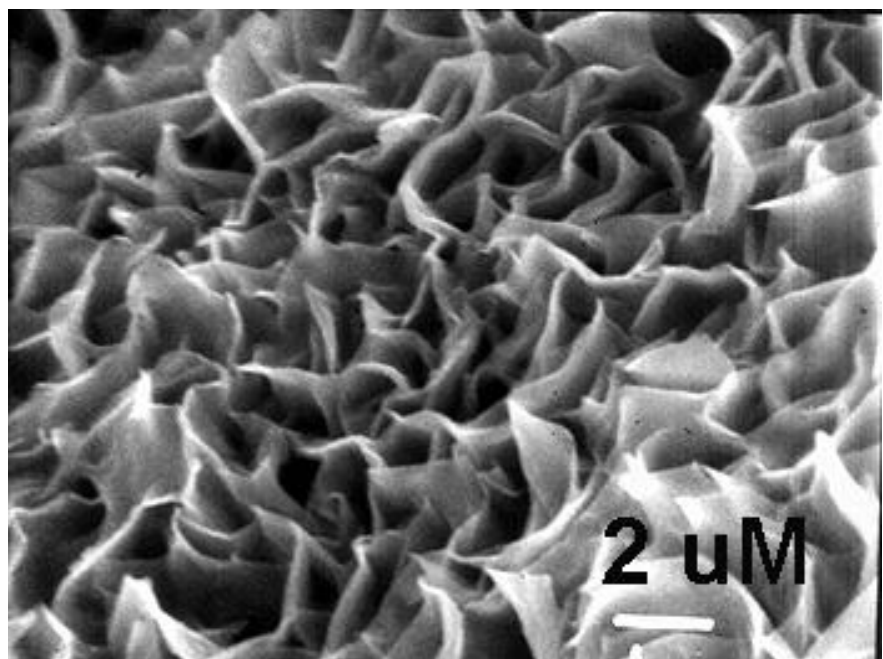




Kaolinite



Illite



Montmorillonite



Varved Clay

Effective Stress Concept

In soil mechanics we are dealing with an idealized continuum, for which analytical solutions are complex, if they exist at all. An important working hypothesis introduced by Terzaghi (1943) is the notion of effective stress, defined as:

"the effective stress represents the part of the total stress, which produces measurable effects such as compaction or an increase of shearing resistance".

- The effective stress, total stress and pore water pressure are related through

$$\sigma' = \sigma - u_w$$

- Some authors start with the expression $\sigma' = a\sigma_s = \sigma - (1-a)u_w$ and impose $a \rightarrow 0$, implying point contacts.
- Effective stress is not a real stress but rather a convenient tool to describe that portion of the total stress that is directly related to a soil's deformation and strength. In other words, effective stress is a convenient book-keeping device.

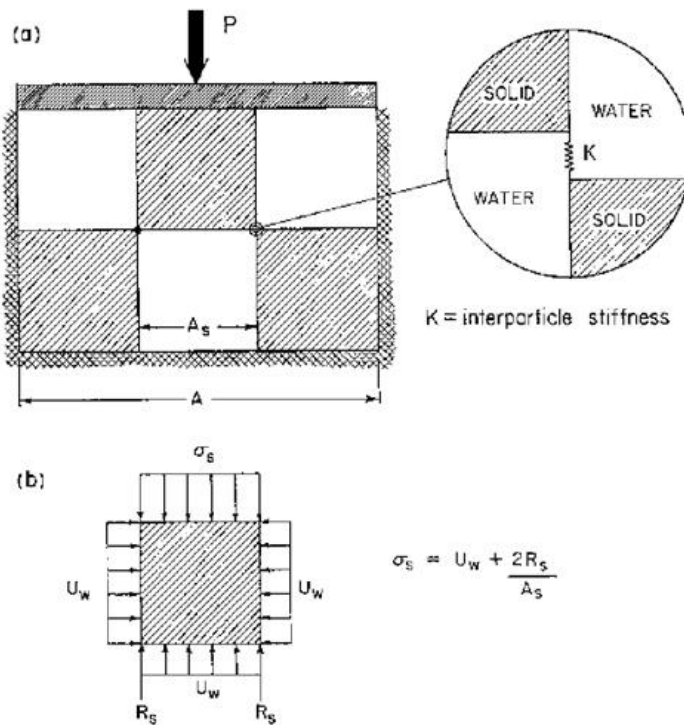


Figure 1: Idealized soil structure under one-dimensional loading.

Geostatic Stresses – Stresses due to self weight

Given that $\sigma_v = \gamma z$ is the vertical stress due to unit weight γ , the effective stress is given by $\sigma'_v = \gamma' z$ where γ' is the buoyant unit weight. For the case of a horizontal surface, the horizontal effective stress is $\sigma'_h = K_o \sigma'_v$, with K_o being the *coefficient of lateral earth pressure*. For a normally consolidated soil: $K_o = 1 - \sin \phi'$.

- granular soils: $0.4 \leq K_o \leq 0.6$
- normally consolidated clay: $0.4 \leq K_o \leq 0.6$
- squeezing rock $K_o > 1$

Stresses Due To Surface Loads

Stress in a soil mass increases when it is loaded at the surface. Since a soil mass is generally a coherent body, continuum mechanics principles are applied. Details into the theory of elasticity, which forms the basis of classical solutions to stress distributions in soils, are beyond the scope of this course. As far as foundation design is concerned, it is important to recognize that stresses are related to strains, and strictly speaking, the deformations are related to effective stresses.

An important equation to predict stress increase is Boussinesq's point load solution for a materially isotropic, homogeneous, elastic halfspace:

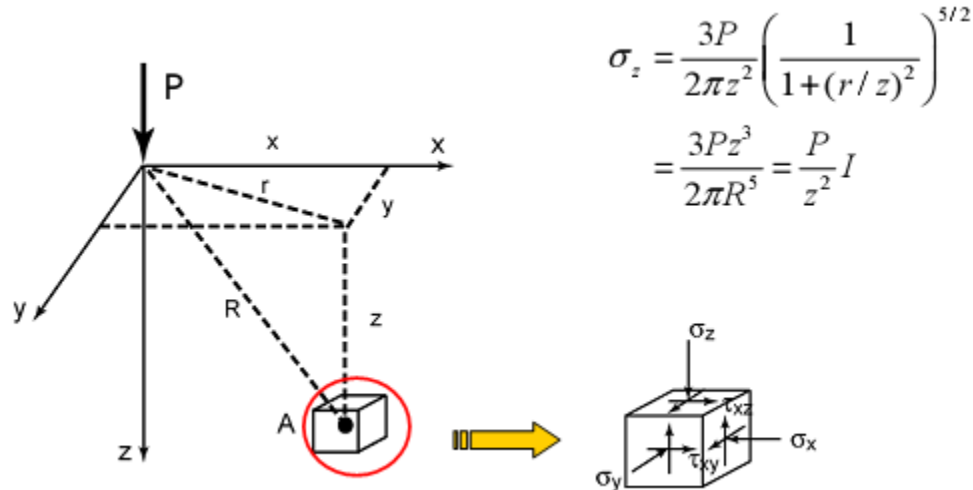


Figure 2: Stress increase due to points load.

Similar equations exist for radial and shear stress components. An important observation is that the stresses are independent of material properties. To predict vertical stress increases to surface loading of arbitrary shape, this solution can be convoluted.

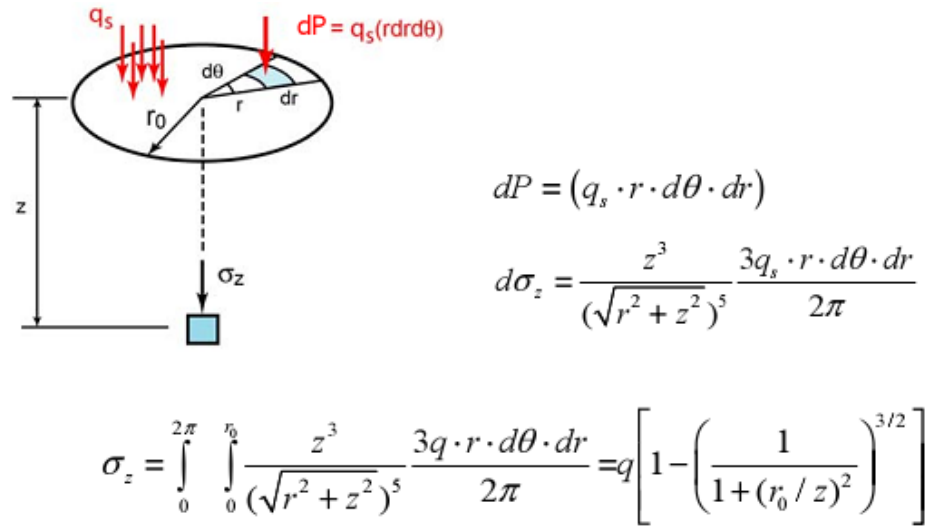


Figure 3: Stress increase due to circular load.

Owing to the complexity of the solutions, influence charts have been developed to estimate stress increases off the centerline, taking into account that the solutions are independent of material properties. Similar equations exist for radial and shear stress components.

In order to estimate vertical stress increase due to a uniformly distributed surface load, the 2:1 rule is often used:

$$\sigma_z = \frac{P}{(B+z)(L+z)}$$

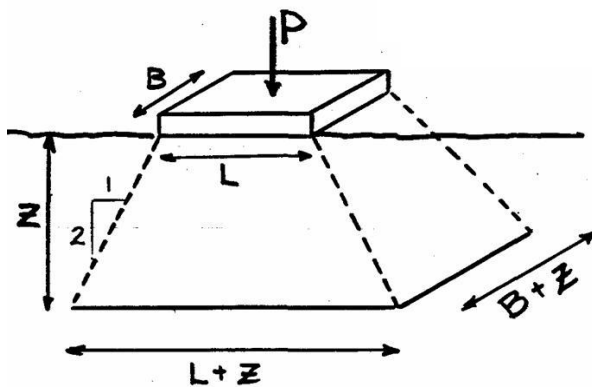


Figure 4: Average stress increase due to rectangular load.

Elastic Settlements

Given stress increases, settlements or deflections can be estimated, for example, under a circular load via:

- Strains: Hooke's Law

$$\varepsilon_z = \frac{1}{E}(\sigma_z - 2\mu\sigma_r); \quad \varepsilon_r = \frac{1}{E}[(1-\mu)\sigma_r - \mu\sigma_z]$$

- Deflections

$$w = \int \varepsilon_z dz + C$$

Most soil bodies are not homogeneous. Nevertheless, if the properties vary slowly, Boussinesq's solutions can still be used to estimate stress increases. To estimate settlement, the integrations are performed numerically taking into account the changes in the stress-dependent properties with depth; i.e.

$$w = \sum_i \frac{1}{E_i} (\bar{\sigma}_z - 2\mu_i \bar{\sigma}_r)_i H_i$$

where H_i represents the thickness of sub-layer i and the bars over the stresses indicate average stress increases.

Table 2: Typical elastic properties.

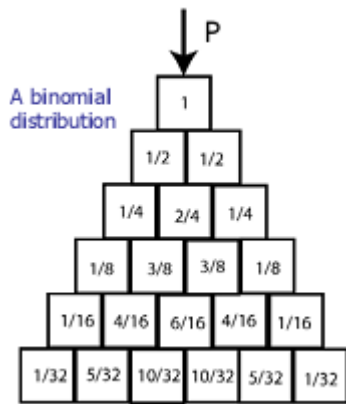
Soil	Poisson's Ratio	E kg/cm ²
Clay	0.4 – 0.5	
Very soft		3 - 30
Soft		20 - 40
Medium		45 - 90
Hard		70 - 200
Sandy		300 - 425
Sand	0.2 – 0.4	
Silty		50 - 200
Loose		100 - 250
Dense		500 - 1000
Sand and gravel		
Dense		800 - 2000
Loose		500 - 1400
Silt	0.3 – 0.35	20 - 200

Note:

- For an isotropic, elastic body only two material properties are required, i.e., the elastic modulus E and Poisson's ratio ν .
- Soils are really not elastic, thus we deal with equivalent elastic materials where the elastic modulus is represented by a secant value. Normally E_{50} is used.
- Most influence charts, such as Newmark's charts, used to estimate stress increase due to surface loads are based on the Boussinesq solution for a point load. His solution does not require material properties.
- More modern stress analysis is based on the application of finite element models that avoid many of the simplifications that have been used for convenience rather than their correctness.

Discrete Particle Approach

An alternative theory to predict stress increase was developed by various investigators to take into account the discrete nature of soil particles.



Force Propagation Model

Assuming a large number of particles, the Gauss function is used:

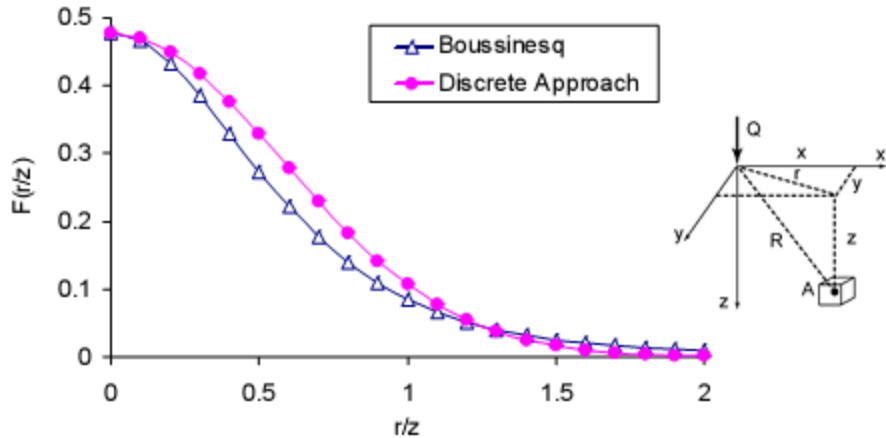
$$S_z = \frac{P}{2\pi\nu z^2} \exp\left(-\frac{r^2}{2\nu z^2}\right)$$

Material property

$$\begin{cases} S_x = \left(\frac{x}{z}\right)^2 S_z \\ S_y = \left(\frac{y}{z}\right)^2 S_z \end{cases} \Rightarrow S_r = \left(\frac{r}{z}\right)^2 S_z$$

$$S_\theta = 0$$

Research into the use of this model has been virtually abandoned since the development of finite element techniques for stress analysis of geotechnical problems. An important observation, however, is that the Boussinesq and Gaussian based equations provide similar vertical stress predictions as shown in the following figure:



$$\text{Given } \sigma_{z\max} = \frac{3P}{2\pi z^2}, S_{z\max} = \frac{P}{2\pi\nu z^2} \Rightarrow \nu = \frac{1}{3} \text{ for } \sigma_{z\max} = S_{z\max}$$

Figure 5: Comparison of Boussinesq and particle theory solutions.

Loading in Excavations

An important assumption in soil mechanics is that the history of stress changes can often be ignored and that only the net increase in loading must be considered when performing settlement analysis. Strictly speaking, this assumption is reasonable if construction is carried out quickly.

$$\sigma_z(\text{net}) = q - \gamma h$$

where h is the depth of excavation and γ is the unit weight of soil.

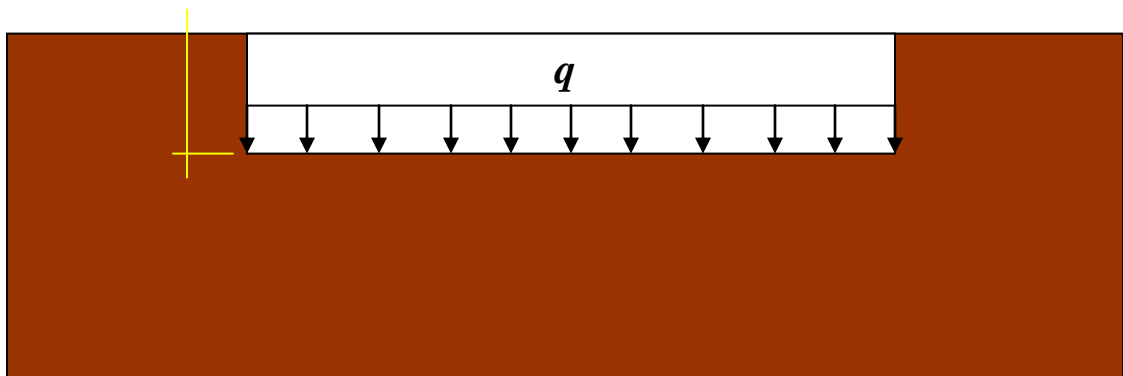


Figure 6: Net stress increase associated with excavation.

Seepage Analysis and Darcy's Law

The strength and deformation characteristics of a soil depend very much on the effective stress, which in turn depends on the pore water pressure. For the case of a static, horizontal water table, the calculations for pore pressure are straight forward. On the other hand, in many applications, the phreatic surface is not horizontal, implying that water is moving. For such situations, a flow analysis must be completed.

According to Darcy's law, the flow rate of the water Q through a porous medium is described by the relation

$$Q = k \frac{H}{\ell} A = k i A$$

where k is the hydraulic conductivity. The *discharge velocity* $q = Q/A$, with the *seepage velocity*, which is the actual velocity, defined as $v_s = q/n$, with n being the porosity.

The heart of seepage analysis is the application of Bernoulli's relation :

$$h = \frac{u_w}{\gamma_w} + z$$

which relates the total head h to the pressure ψ and elevation heads z . Referring to Figure 7, we have water flowing through an isotropic soil under an impermeable concrete dam. The driving force for the flow of water under the dam is head H , which we will divide up into equipotential drops characterized by lines of constant head such that $H = n_e h$. Also shown in the figure are flow lines drawn in such a way that the discharge between flow lines is equal.

According to Darcy's law, the flow in one stream channel is $Q = k \frac{h}{a} b$. Given that we have n_f flow channels that are perpendicular to the equipotentials, the total flow is

$$Q = kH \frac{n_f}{n_e} \frac{b}{a} \quad \text{or} \quad Q = kHS$$

where S is the shape factor. For flow net construction, we usually attempt to keep $b/a = 1$.

Once a flow net has been constructed, one can estimate the pore pressure distribution by using Bernoulli's equation.

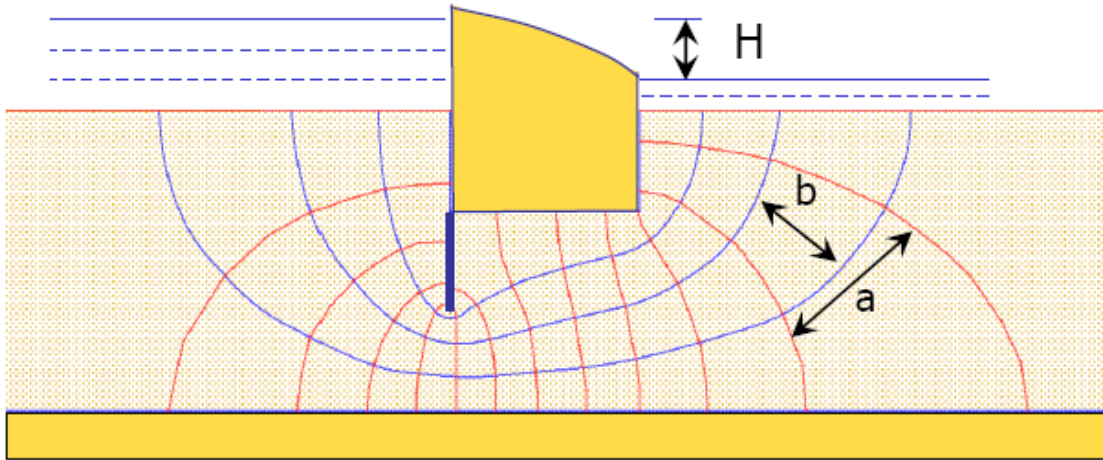


Figure 7: Illustration of seepage analysis.

Consolidation – Compressibility of Clay

Consolidation is the process whereby the water content in a saturated soil decreases leading to time-dependent settlements. The classical means for establishing consolidation settlements is by the *oedometer test*, in which the stress-strain relation is for the case of zero lateral strain.

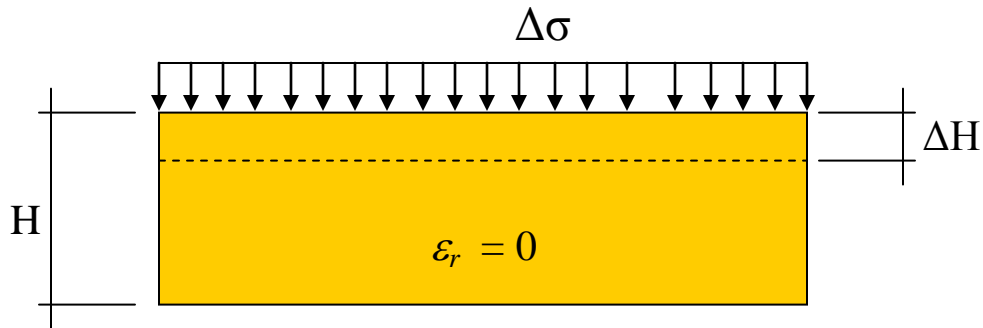


Figure 8: Schematic for geometry of *oedometer test*.

The consolidation test relates the changes in vertical strain to changes in void ratio; i.e.,

$$\Delta \varepsilon_z = \frac{\Delta H}{H} \rightarrow \Delta \varepsilon_z = \frac{\Delta V}{V} = \frac{\Delta e}{1+e}$$

Void ratio is related is function of effective stress via an “equation of state” that depends on stress history as shown in Figure 9.

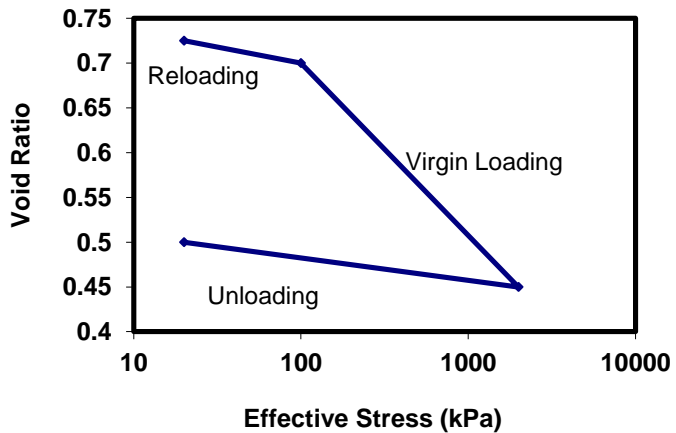


Figure 9: Typical one-dimensional compression relation for clay.

For the one-dimensional case, $\Delta\sigma' \approx 0$ immediately after the load is applied, but increases as excess pore pressure is dissipated; i.e., for $\Delta\sigma = 0 \Rightarrow \Delta\sigma' = -\Deltau_w$. As the effective stress increases, water squeezes out resulting in a change of void ratio.

Note the following terms:

- 1) Coefficient of volume change – $m_v = -\frac{a_v}{1+e}$
- 2) Compression index – $C_c = -\frac{\Delta e}{\Delta \log \sigma'} \text{ (virgin loading)}$
- 3) Recompression index – $C_r = -\frac{\Delta e}{\Delta \log \sigma'} \text{ (reloading)}$
- 4) Preconsolidation pressure – σ'_p , maximum past effective pressure, separating recompression (reloading) and virgin loading.
- 5) The recompression curve is different from the virgin curve due to a redistribution of particles. Given that σ'_o is the initial, in-situ effective stress the ratio $\frac{\sigma'_p}{\sigma'_o}$ is referred to as the overconsolidation ratio (OCR).
- 6) Deformation at constant effective stress is referred to as *secondary compression*. Secondary compression may be considered as a creep phenomenon.

Consolidation Rates (Terzaghi's One-Dimensional Model)

The rate excess pore pressure dissipation can be predicted by using Terzaghi's one dimensional consolidation theory. The basic assumptions inherent in the theory are:

- fluid and solid are incompressible
- soil is saturated
- soil is homogeneous
- Darcy's Law is applicable
- one dimensional fluid flow
- one dimensional strain (small)

The rate of pore pressure dissipation is given by

$$\frac{k}{m_v \gamma_w} \frac{\partial u_w^2}{\partial z^2} = \frac{\partial u_w}{\partial t} - \frac{\partial \sigma}{\partial t} \quad \Rightarrow \quad c_v \frac{\partial u_w^2}{\partial z^2} = \frac{\partial u_w}{\partial t}$$

for the incremental test where with $\dot{\sigma} = 0$, with c_v being *the coefficient of consolidation*.

The *degree of consolidation* is defined as

$$U_z = \frac{e_o - e}{e_o - e_f} \quad \Rightarrow \quad U_z = 1 - \frac{u_w(z, t)}{\Delta \sigma}$$

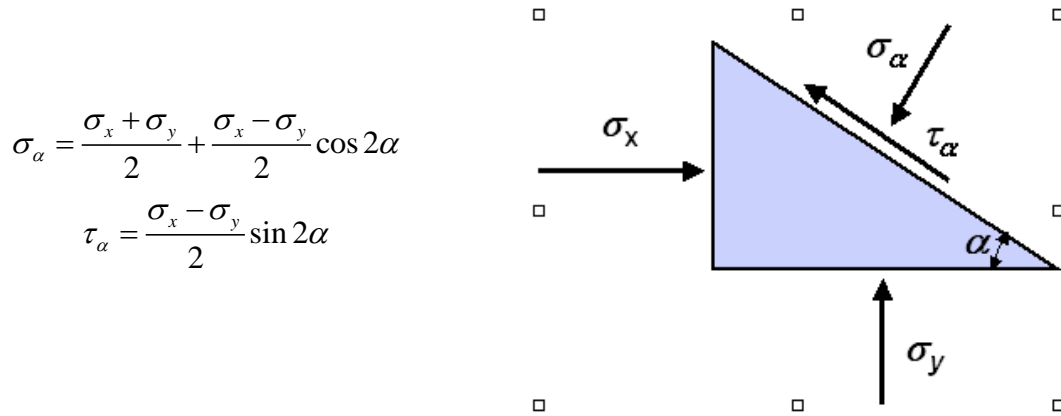
after linearizing relation between void ratio and stress changes. Assuming linearization, the time-dependent settlement is

$$\Delta H(t) = U_{ave}(t) \Delta H .$$

Mohr's Circle and Stress Transformations

Much progress in our understanding of soil behaviour has come about by performing **triaxial tests**, in which the principle stress orientations are lined up with the horizontal and vertical planes. More correctly, the principal stresses correspond to the axial and radial orientations. This is not the situation in the **direct shear test** (presented later) or for general planar states of stress. While soil mechanics problems tend to be 3D in nature, we often can simplify and use 2D idealizations. For such idealizations, Mohr's circle transformations are valuable. This section briefly reviews stress transformations within the context of graphical procedures for geomechanics problems. Compression is assumed to be positive.

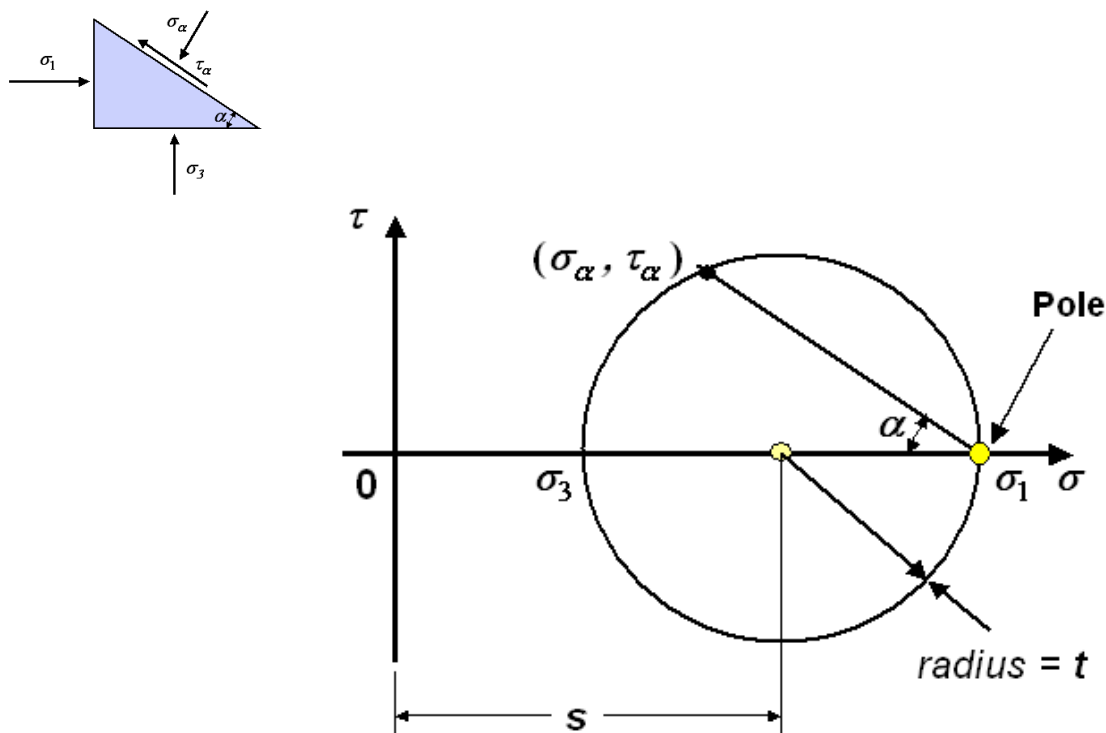
Taking equilibrium of the soil element shown in the figure yields the following stresses on the plane that is at an orientation α with respect to the horizontal plane. The principal planes are assumed to align themselves with the co-ordinate axes. An examination of the transformation equations indicates that they contain the center of the Mohr's circle ($s, 0$) as well as its radius t . The stress combination (s, t) , which corresponds to the stress pair at maximum shear, represents stress invariants for planar analysis.



The transformation equations can be combined to form Mohr's circle (shown on the following page), which fully defines the state of stress at a point. Referring to the figure, we can graphically determine the stress at any orientation α by the following process:

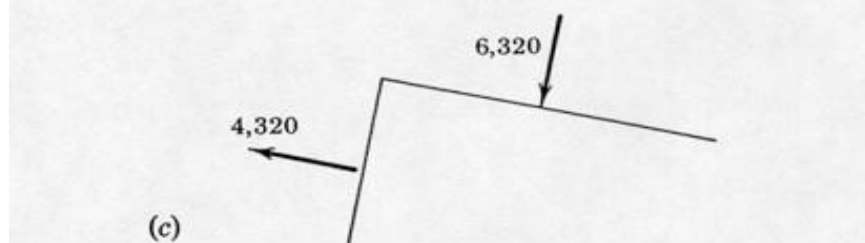
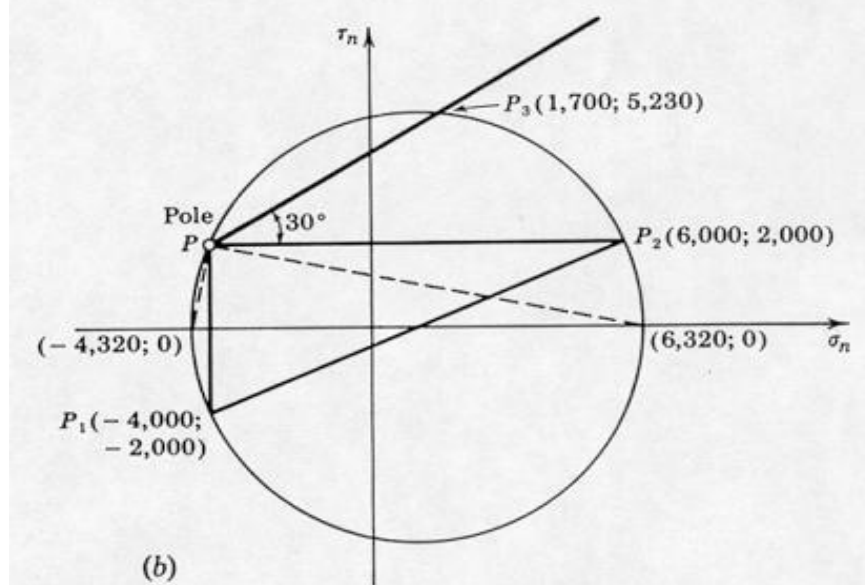
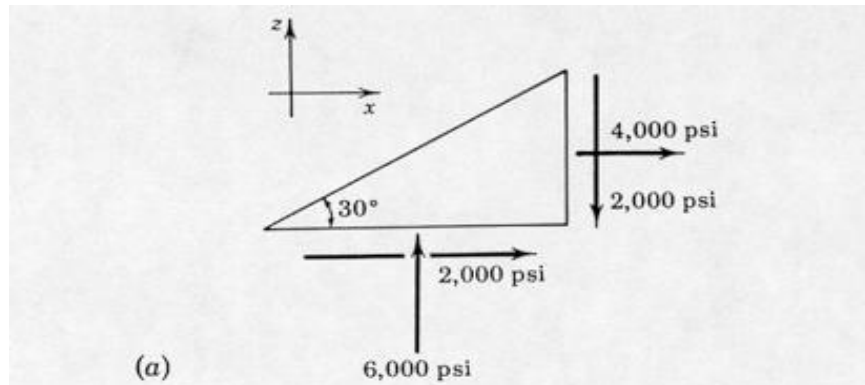
- Given that the vertical stress, which corresponds to σ_3 , plot its value on the σ -axis and draw a line through the stress point parallel to the plane on which the stress acts; i.e., for this point the line follows the axis.
- Repeat the same for σ_1 . This time the line passing through the stress point is parallel to the τ -axis.

3. The intersection of the lines drawn for steps 1 and 2 intersect a point referred to as a **pole**, which represents the *origin of planes*.
4. In order to find the stresses on plane α , draw a line parallel to this plane passing through the pole. The point where the line intersects the circle provides the values for the normal and shear stresses $(\sigma_\alpha, \tau_\alpha)$. The sign convention corresponding to positive stress values is shown in the small free-body diagram to the left. A positive shear is defined as one causing a counter-clockwise rotation about a point that is on the inside of the triangle.



While the procedure shown here was demonstrated using the stresses on the principal planes, the same procedure can be used for any combination of known stresses. For the more general case, the pole will not lie on the σ -axis.

Example: Find the magnitude and orientation of the principal stresses for the following problem using the method of poles.



Shear Strength

An important consideration in geotechnical engineering is the stability of the foundations, retaining structures, tunnels and slopes, including embankments. In order to make assessments regarding stability, the strength of the material is required, more specifically, the shear strength of soil. Various tests exist to determine shear strength, the two most common being the *direct shear test*, shown in Figure 1, and the *triaxial test*, shown in Figure 2. Table 1 compares the two tests.

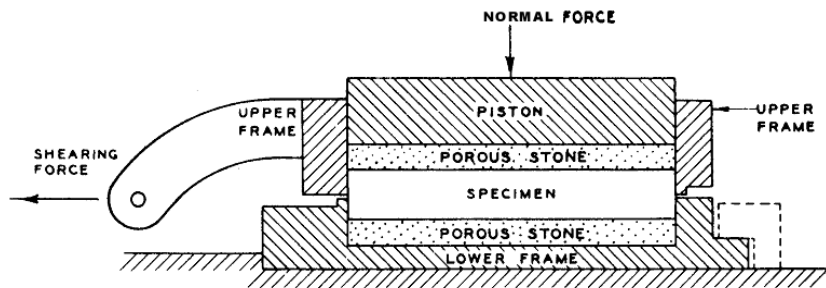


Figure 1: Schematic of direct shear test.

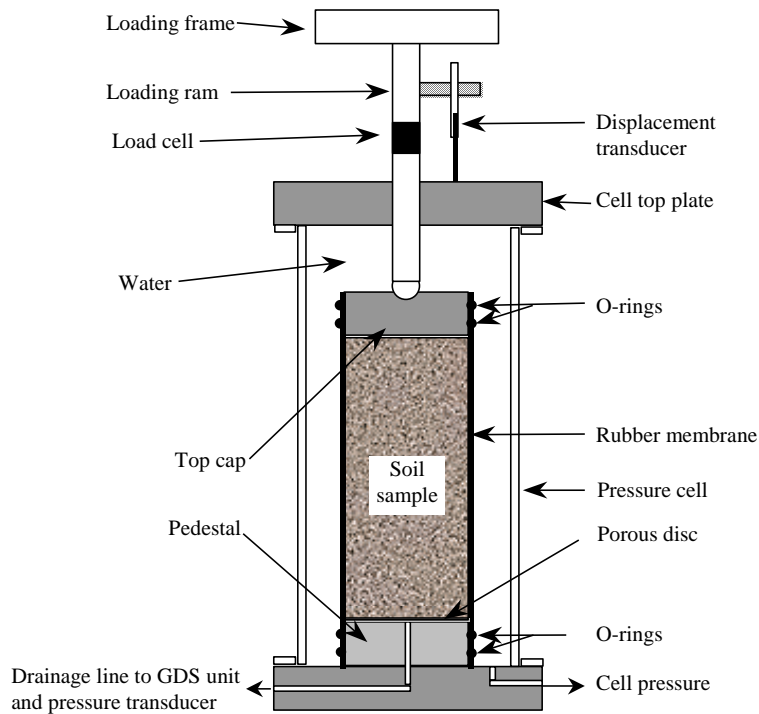


Figure 2: Triaxial test set-up for resilient modulus with specimen fabrication accessories.

Table 1: Comparison of direct shear and triaxial tests.

Test	Advantages	Disadvantages
Direct Shear	<ul style="list-style-type: none"> Simple to set up and perform, keep only track of shear force T, normal force N and corresponding displacements x and y. For sand we have $T = \mu N$ Good estimate of residual strength 	<ul style="list-style-type: none"> Plane of failure predetermined as shown in Figure 3 Cannot control drainage Do not know state of stress until failure Stress concentrations leading to progressive failure
Triaxial	<ul style="list-style-type: none"> Greater flexibility in stress control State of stress always known Failure not on predetermined plane Control of pore pressure 	<ul style="list-style-type: none"> Equipment is more complex

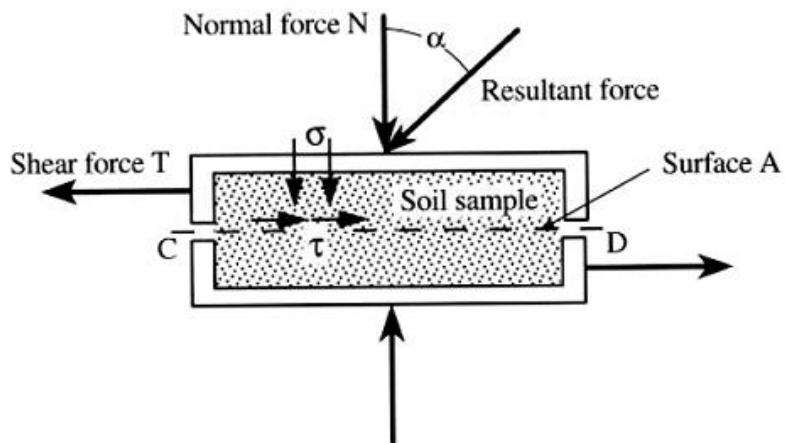


Figure 3: Predefined failure plane in a direct shear test.

Mohr-Coulomb Failure Criterion

The backbone of describing shear strength is the Coulomb (1776) failure criterion

$$\tau_f = c + \sigma_f \tan \phi$$

in which c represents the soil's cohesion, ϕ is the material's friction angle as depicted in Figure 4, and the subscript f denotes the combination of shear stress and normal stress on the failure plane. The direct shear test can be used to directly determine the strength parameters along a predefined failure plane.

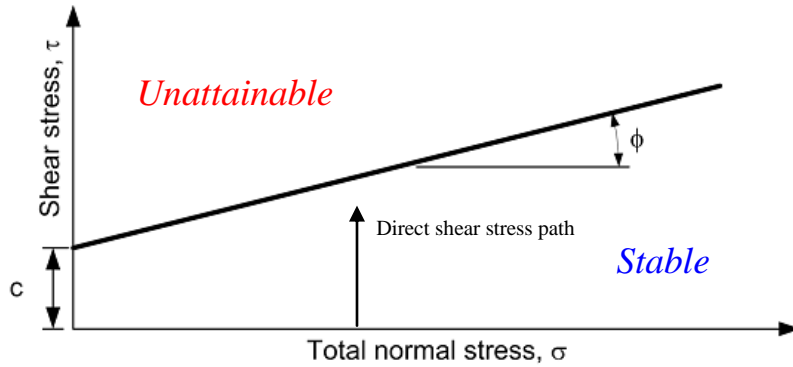


Figure 4: Coulomb failure criterion.

Since the failure of soils depends on effective stress, a more appropriate statement of failure is

$$\tau_f = c' + \sigma'_f \tan \phi'$$

where c' is the cohesion and ϕ' frictional angle and the primes denote that parameters correspond to effective stresses.

For more general states of stress, Mohr suggested that failure is imminent once the Mohr's circle touches a failure envelope; i.e. $\tau_f = f(\sigma_f)$. Within the context of soils, it is assumed that the intermediate principal stress does not influence failure. Figure 5 shows the relation between principal stresses at failure. The failure plane makes an angle of $\theta = 45 + \phi'/2$ with respect to the major principal plane.

Taking into account the geometric relations, failure conditions may also be expressed in terms of principal stresses as

$$\sigma_1 = K_p \sigma_3 + 2c' \sqrt{K_p}$$

with

$$K_p = \frac{1 + \sin \phi'}{1 - \sin \phi'}$$

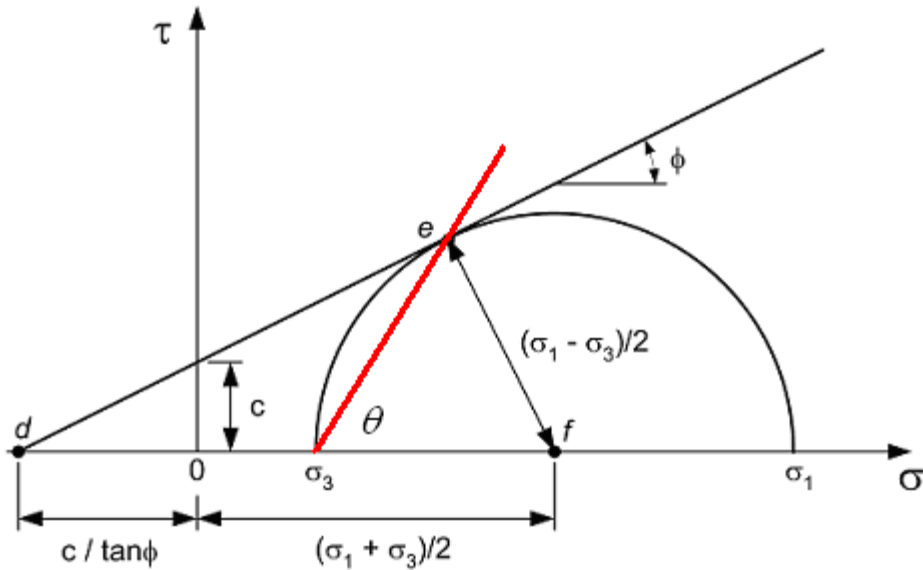


Figure 5: Failure when Mohr's circle touches Coulomb failure envelope.

Obliquity Consideration

Consider the average stresses between the block of wood and the flat surface shown in Figure 6.

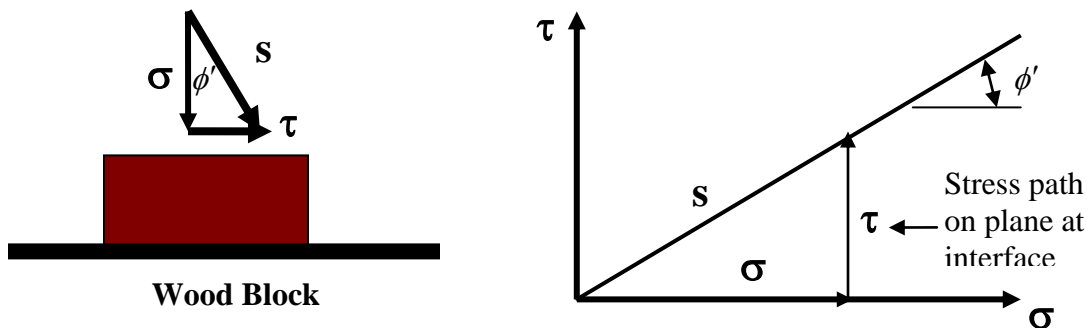


Figure 6: Demonstration of obliquity relation.

Given that $\tan \alpha = \tau/\sigma$, as long as $\alpha < \phi'$, the block of wood will not move (stable). The angle α is referred to as the angle of obliquity of the stress vector \vec{s} . It depends on the state of stress and is not a material property. The condition for incipient slip is defined as $\alpha = \phi'$. When performing a **direct shear test** on a soil, the notion of obliquity is directly

transferable to the failure of soil as the failure plane is predefined, as demonstrated in Figure 3.

A factor that does not enter the situation, in which we slide a block of wood over a flat surface is the effect of changing state of the material. For the soil, some of the energy goes into forcing the material to undergo volume change, with the remaining energy going toward overcoming friction.

Let us consider the following energy balance:

$$T\Delta x = T_{friction}\Delta x + N\Delta y \Rightarrow \tau = \tau_{friction} + \sigma \frac{dy}{dx}$$

in which $\tau_{friction}$ is the shear stress under zero volume change, y is the vertical displacement and x is the horizontal shear displacement. Figure 7 clearly shows that the shear stress overcoming friction is less than the measured value; i.e., some of strength is due to forcing dilation.

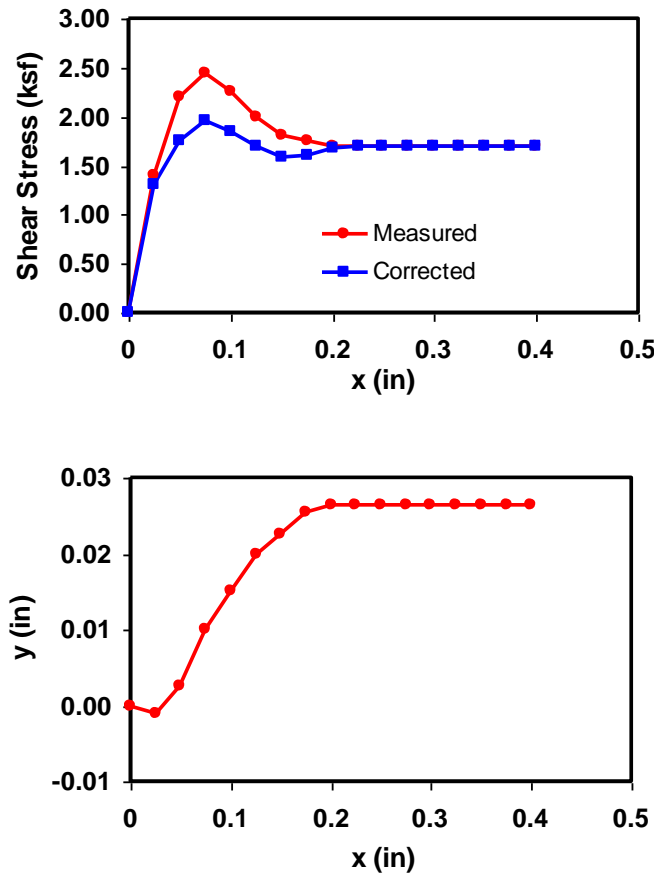


Figure 7: Direct shear results including energy correction.

Figure 8 presents the failure envelopes for the case of a material that dilates and one corresponding to zero volume change. The latter case provides the strength when only friction acts to provide stability.

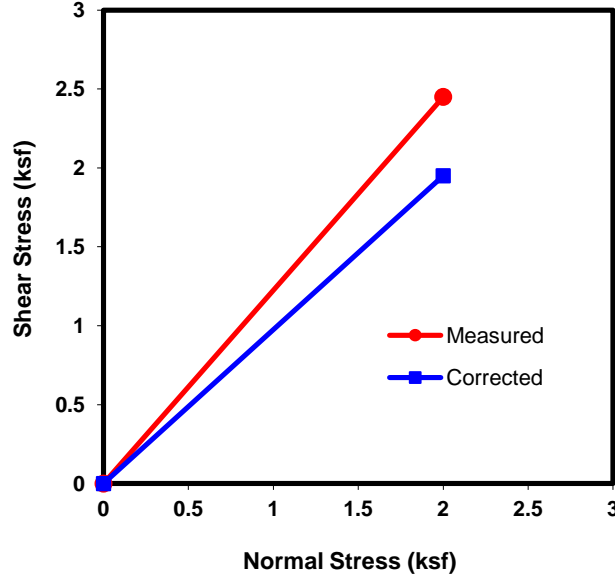


Figure 8: Failure envelope for direct shear test results.

It should be noted that the full state of average stress is known in a direct shear sample at failure, as shown in Figure 9.

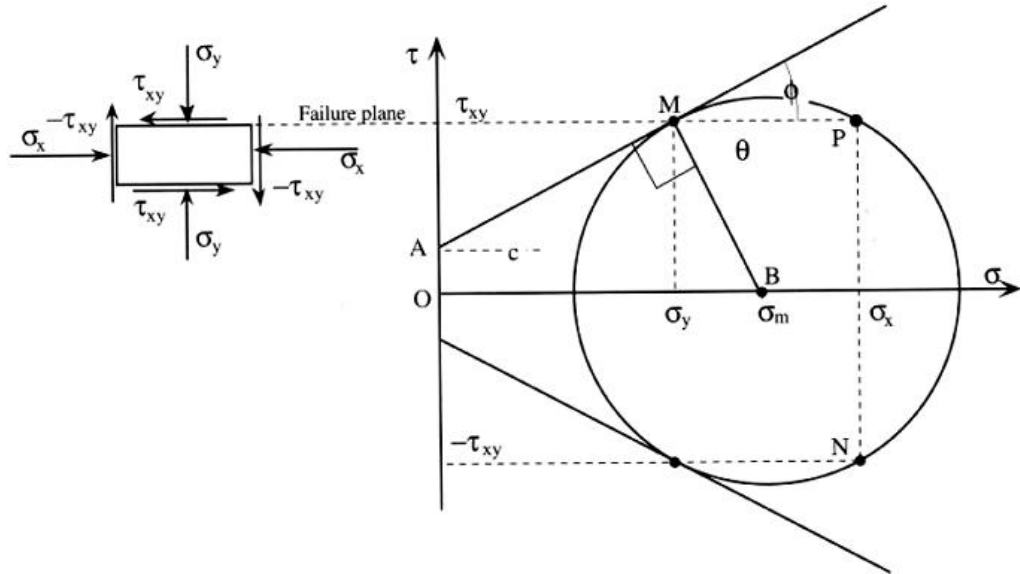


Figure 9: State of stress in direct shear box at failure using the origin of planes.

Obliquity Relation for Triaxial Test

Consider now a similar problem for a state of stress at a point in a granular soil. The resultant stress on a plane at an angle θ with respect to the major principal stress plane is given by \bar{s} , with its magnitude defined as $s = \sqrt{\sigma^2 + \tau^2}$. It can be seen that the maximum obliquity α_{max} occurs when \bar{s} is tangent to the Mohr's circle.

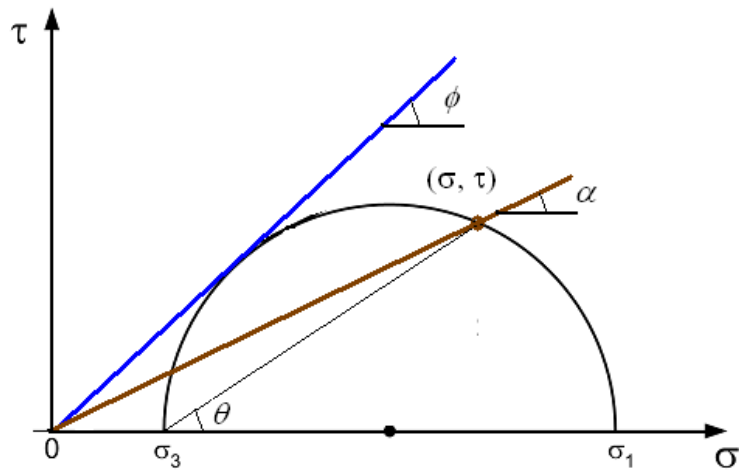


Figure 10: Obliquity considerations for triaxial test.

In other words, failure occurs for $\alpha_{max} = \phi'$ or $(\tau/\sigma)_{max} = \tan \alpha_{max}$.

For a triaxial test, the maximum obliquity at any instant may be expressed in terms of triaxial stress invariants as

$$\left(\frac{t}{s'} \right)_{max} = \frac{\sigma'_1/\sigma'_3 - 1}{\sigma'_1/\sigma'_3 + 1} = \sin \alpha_{max}$$

implying failure with $\alpha_{max} \rightarrow \phi'$ at failure.

Triaxial Test Stress and Strain Invariants

Most advances in the understanding of the deformation and strength characteristics of soils has been attained via triaxial testing programs, in which stresses are applied to an axially symmetrical sample via cell pressure ($\sigma_r = \sigma_c$), to provide confinement and an

axial load that imparts a deviator stress ($q = \sigma_d$) yielding total axial stress σ_a ($= \sigma_c + \sigma_d$). Figure 11 illustrates a modern test setup.

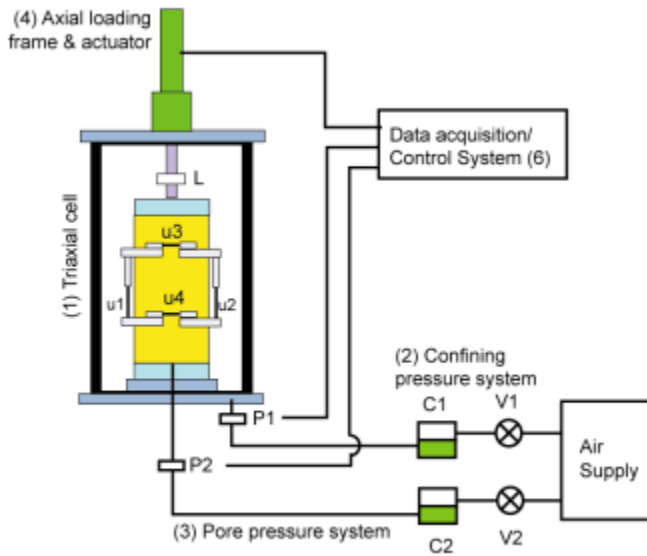


Figure 11: Schematic of triaxial test.

The success of this apparatus lies in the ability to control and measure the pore pressure (u_w) independently.

Assuming the convention, in which compression is positive, the incremental strain energy per unit volume within the soil sample is given by,

$$dU = \sigma_a d\varepsilon_a + 2\sigma_r d\varepsilon_r$$

By considering energy equivalence, two sets of triaxial stress invariants are introduced:

$$\begin{aligned} s &= \frac{1}{2}(\sigma_a + \sigma_r) & \Rightarrow & \quad d\varepsilon_v = d\varepsilon_a + 2d\varepsilon_r \\ t &= \frac{1}{2}(\sigma_a - \sigma_r) & \Rightarrow & \quad d\varepsilon_t = d\varepsilon_a - 2d\varepsilon_r \end{aligned} \quad (\text{MIT})$$

and

$$\begin{aligned} p &= \frac{1}{3}(\sigma_a + 2\sigma_r) & \Rightarrow & \quad d\varepsilon_v = d\varepsilon_a + 2d\varepsilon_r \\ q &= \sigma_a - \sigma_r & \Rightarrow & \quad d\varepsilon_q = \frac{2}{3}(d\varepsilon_a - d\varepsilon_r) \end{aligned} \quad (\text{Cambridge})$$

The stress invariants for the first set correspond to center and radius of Mohr's circle (Figure 12), whereas for the second set, p is the true average stress with q representing the deviator stress. Each set of invariants has its advantages and disadvantages.

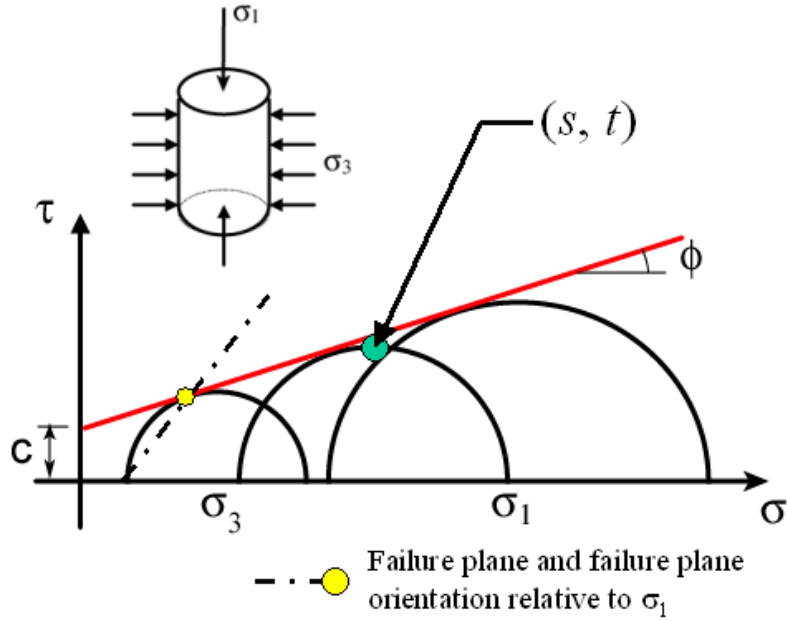


Figure 12: Schematic definition of (s, t) and Mohr-Coulomb failure criterion.

Stress Space

The $\tau - \sigma$ space is convenient for two-dimensional problems since it allows use of Mohr circle construction for interpreting the orientation of the principal states of stress, maximum shear, etc. On the other hand the $s-t$ representation defines the stress conjugates corresponding to maximum shear stress as shown in the previous figure. The advantage of using this representation is that one need only keep track of one point rather than an entire circle as the state of stress changes and as demonstrated in Figure 13, it is easier to fit a line to points than to identify a line that best fits potential tangents. The failure criterion within this stress space is given by

$$t_f = a' + s'_f \sin \psi'$$

where $a' = c' \cos \phi'$ and $\tan \psi' = \sin \phi'$. The critical plane still corresponds to (σ'_f, τ_f) . Although not emphasized here, the failure envelope is often a little curved and we attempt to linearize the criterion over an interval of interest as shown in Figure 14. Curved failure surfaces are not unusual for cohesionless soils.

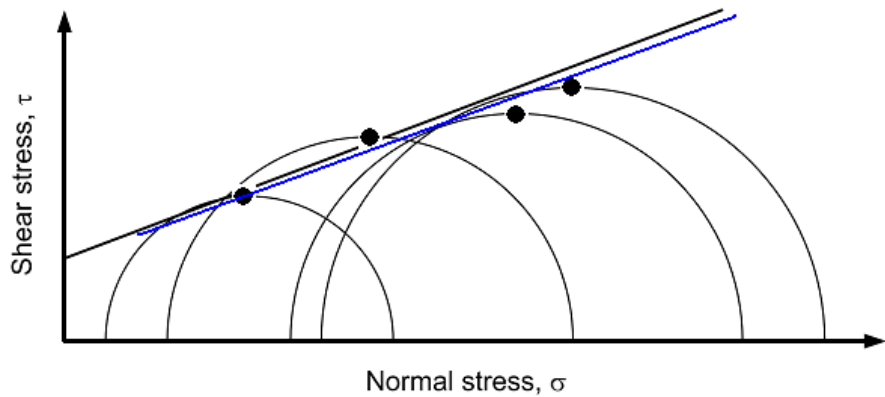


Figure 13: Schematic for fitting failure surface to experimental data.

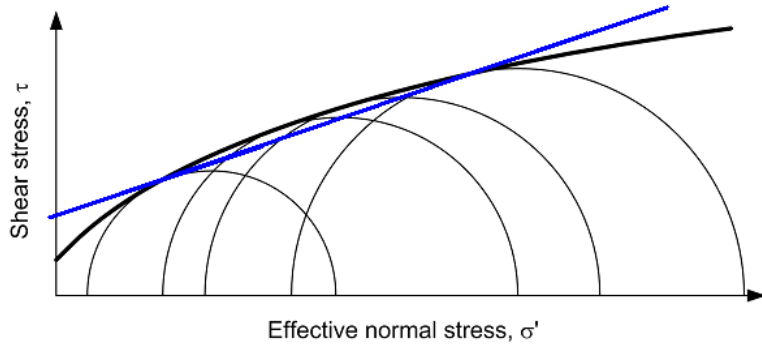


Figure 14: Linearization of a curved failure surface.

Drainage Conditions for Triaxial Test

Typical triaxial tests have two stages of loading: ***consolidation stage*** where the cell pressure is increased and the sample may either be allowed to drain (**C**) or drainage may be prevented (**U**); and the ***shear stage***, which may also drained (**D**) or undrained (**U**). Figure 15 summarizes typical stages. Given that one has control of drainage, triaxial tests may be performed according to the following drainage conditions: **UU** – unconsolidated and undrained; **CU** – consolidated and undrained; and **CD** – consolidated and drained. The **UU** test, sometimes referred to as the quick test, is normally carried out on clays; the **CU** test, which includes pore pressure measurement corresponding to constant volume, is also performed on clays; and **CD** test with volume change measurement is best suited for cohesionless materials. **CU** tests are often not successful when dealing with dense sands due to fluid cavitating under high tension. **CD** tests are often not practical for cohesive soil due to the length of time it takes to complete a test (one to two weeks) as a result of low hydraulic conductivity.

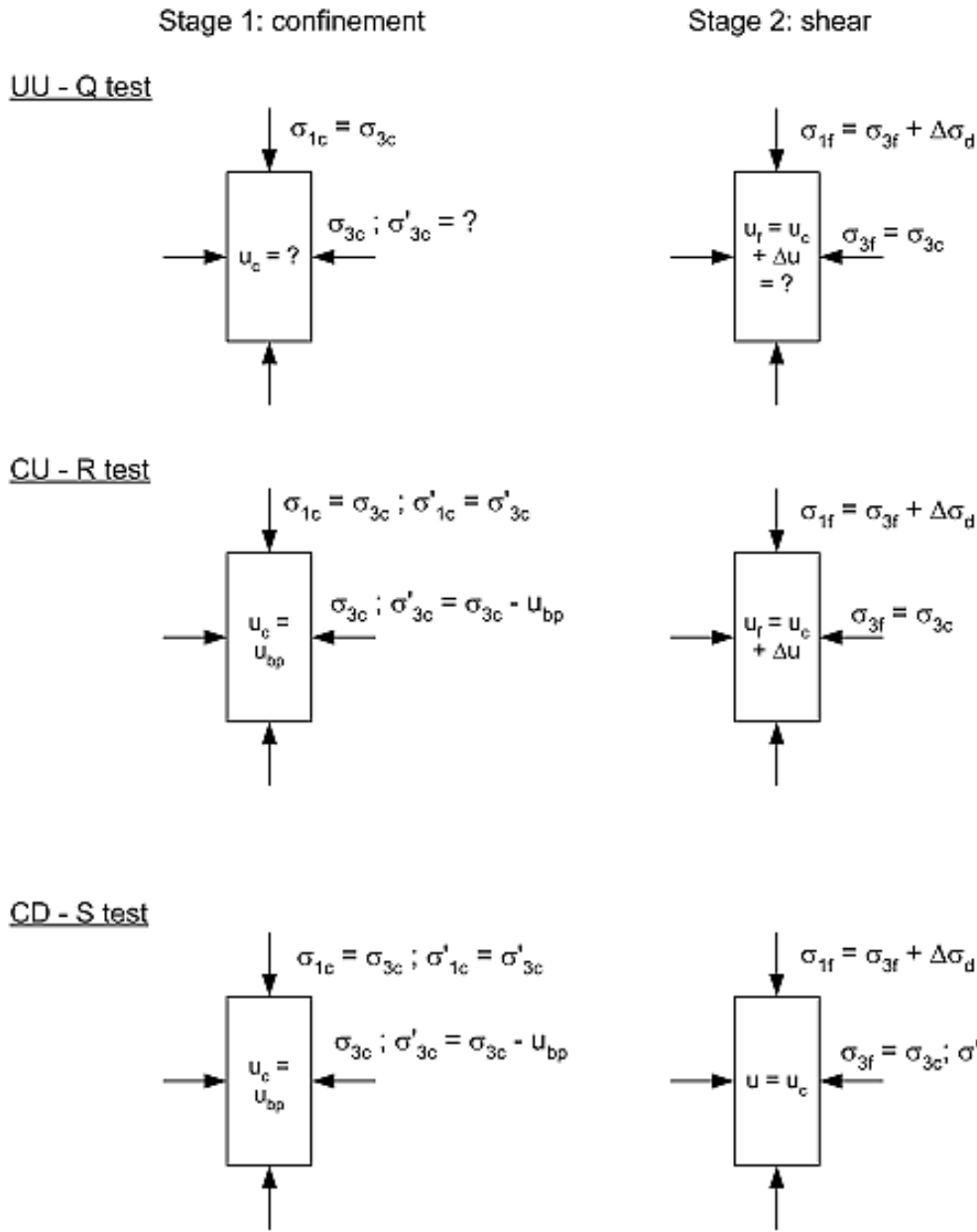


Figure 15: Three typical triaxial testing sequences.

Loading Conditions for Triaxial Test

During the shearing stage, the following drained stress paths (see Figure 16) are encountered:

- **AC** – Axial compression, where cell pressure is constant and a axial load is increased via the loading rod such that $\Delta t/\Delta s = 1$

- **AE** - Axial extension, where cell pressure is constant and a axial load is decreased via the loading rod such that $\Delta t/\Delta s = -1$
- **LC** – Lateral compression, where cell pressure is increased and a axial load stays constant such that $\Delta t/\Delta s = -1$
- **LE** - Lateral extension, where cell pressure is decreased and a axial load stays constant such that $\Delta t/\Delta s = 1$

A stress path is a locus of points that defines the changes in stress during a loading history. This is most often completed using (s, t) invariants or (p, q) invariants. There are three common stress paths:

- **TSP** - Total stress path
- **TSSP** – Total stress path minus static (initial) pore pressure
- **ESP** – Effective stress path – total stress minus total pore pressure, which may consist of initial pressure plus excess pore pressure developed during the shearing of the sample.

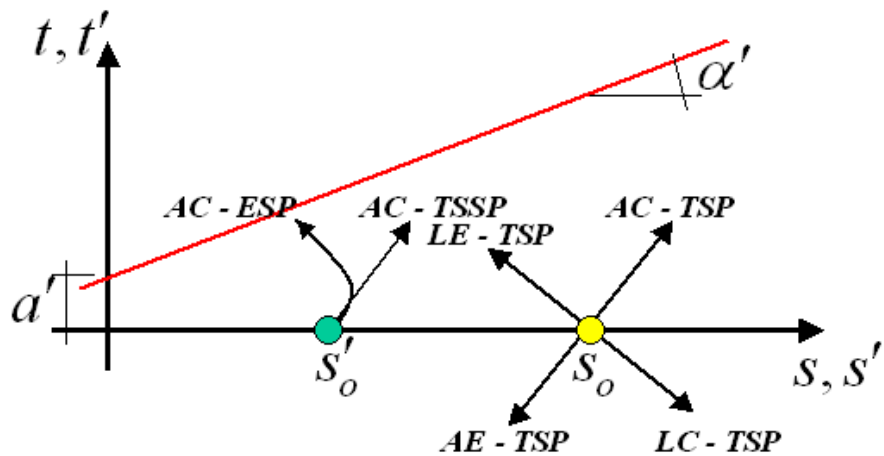


Figure 16: Schematic definition of stress paths as well as failure envelope in (s, t) space.

When referring to Figure 16, one should note that all the stress paths start from the s -axis, which is typical for most routine triaxial tests. On the other hand, the stress paths *in-situ* start from the K_o line, which in terms of the triaxial stress invariants is defined as

$$t = \frac{1 - K_o}{1 + K_o} s'$$

Shear Strength of Sand

Sand develops shear strength as a result of particle interlock and intergranular friction. These depend in turn on the soil gradation and density, as well as on the roughness and angularity of the particles. At high confining pressures, particle crushing is also important.

Drained Strength

Owing to the high permeability of cohesionless soils, for most loading cases, the developed strength is based on drained conditions. Exceptions include: earthquake loading; blasts; etc. Depending on whether the material is dense or loose, the volume of the specimen may either increase or decrease as the shear (deviatoric stress) is applied, as shown in Figure 1. At high confinement, a dense sample may however show loose sample deformation characteristics, with a loose sample showing dense sample traits (volume increase) at low confinement.

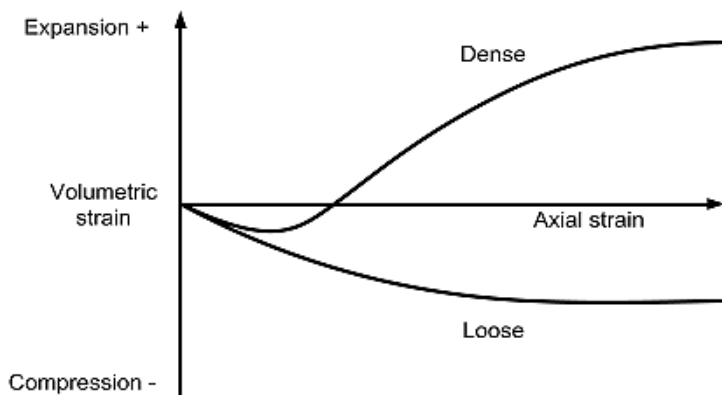
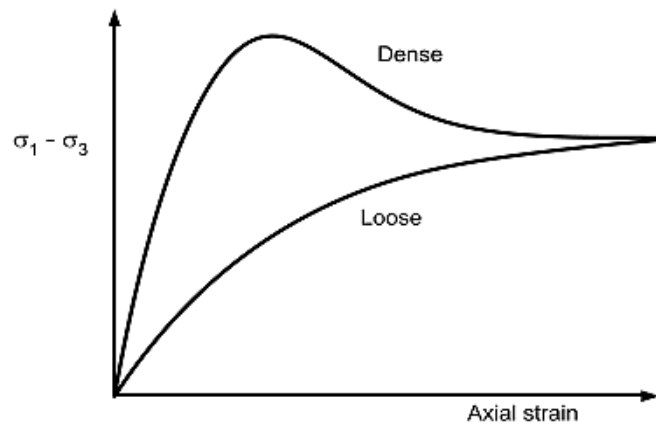


Figure 1: Triaxial test results for drained conditions.

A state line, referred to as the critical state line, exists that relates a critical void ratio to confinement. Depending on the investigator, the critical void ratio can either refer to the initial value or that value at failure. Figure 2 shows a schematic of the critical state line. Under drained conditions, void ratio changes depend on the initial state of the sand. For undrained conditions, the void ratio stays constant and the effective stress changes. For a loose material, the effective confinement decreases, which could initiate failure.

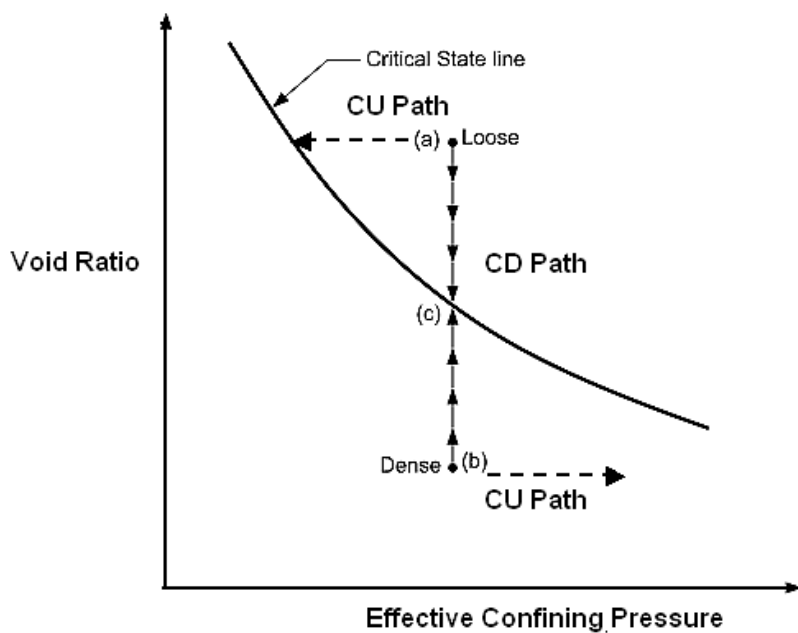


Figure 2: Volume change characteristics depending on initial state of material.

Similar to the direct shear results, an energy correction can be applied to separate shear strength due to dilation characteristics and those due to shear.

Liquefaction and Cyclic Mobility

Undrained Behaviour - The following figure gives the stress-strain behaviour of sand that is loaded incrementally under CU or CD static conditions.

Soil A liquefies due to the excess pore pressure reducing the effective stresses to zero. The denser soils do not undergo a shear strength loss as great as that observed for the loose sand. Soil B temporarily loses some strength, only to gain strength at higher strains. Soil C continuously gains strength. *Liquefaction* can occur under static

(monotonic) loading if the permeability of a soil is low enough when compared with loading rate as to induce positive pore pressures, which reduce the effective stress to zero.

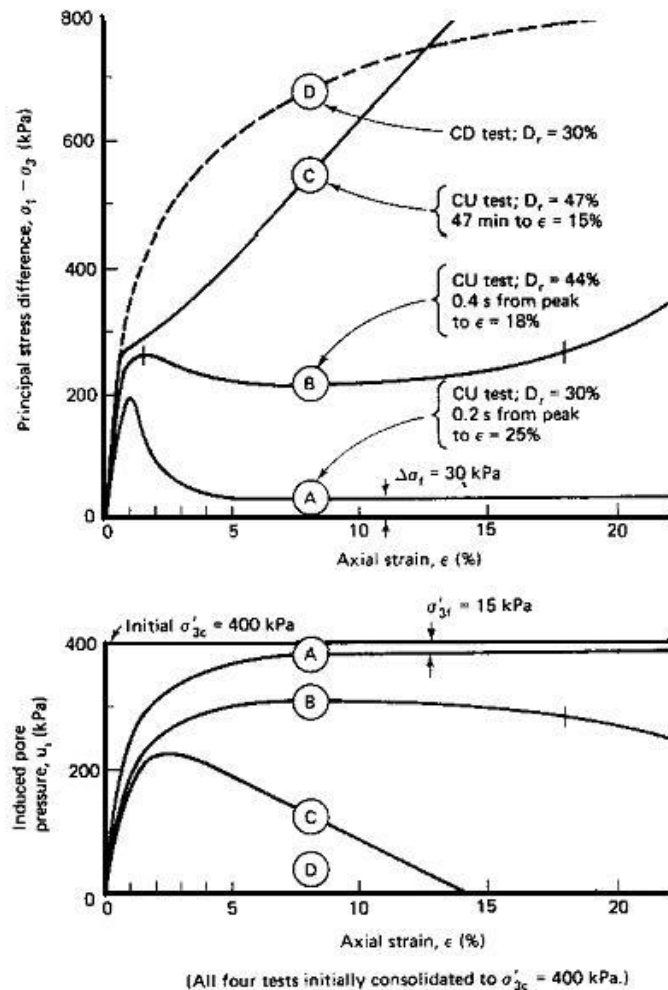


Figure 3: Undrained behaviour of sand.

Liquefaction - Liquefaction is the loss in shear strength of a cohesionless soil due to the buildup of high excess pore pressures, usually the result of impulse loading, resulting in exceptionally large strains under small stresses. Loose sands are most susceptible to liquefaction.

Cyclic Mobility (Observed in laboratory samples) - Both dense and loose soils can liquefy when loaded cyclically. During cyclic mobility, cyclic loads can cause a buildup of positive pore pressures in medium to high density soils and induce measurable strains in sands that ordinarily exhibit a dilative response under static loads.

Surprisingly, dense soils can liquefy. However, it should be noted that even though effective confining stresses momentarily are zero, the specimen can withstand additional cyclic loading. Strains are smaller than for loose sample and complete collapse does not occur.

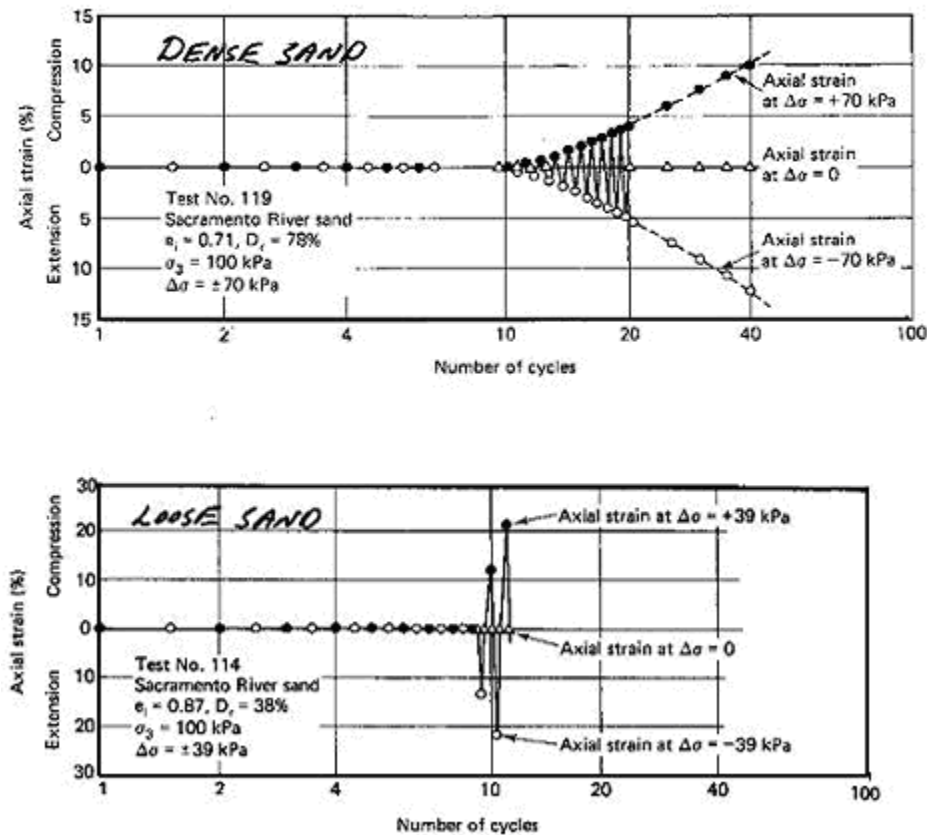


Figure 4: Cyclical undrained response of sand to constant deviatoric stress amplitude.

Shear Strength of Clay

The strength of clay, which depends on the rate of loading and temperature, is more complex than that of sand. Clays, which originally appear stable, can become unstable due to the soil skeleton creeping. The more complex behaviour is largely due to the water, some of which is responsible for the clay's structure. If clay has a previous history then it often remembers the history.

Unlike sand, clay possesses some cohesion. When normally consolidated, the amount of cohesion is quite small. If the material is pre-consolidated to a higher stress level σ'_c , the clay minerals re-orientate themselves to new equilibrium positions and develop a higher level of cohesion that appears to increase with an increase in pre-consolidation pressure. Figure 1 illustrates the transition from over-consolidated to normally consolidated failure.

The shear strength of clay depends on the clay minerals, water content, drainage condition and initial state of stress.

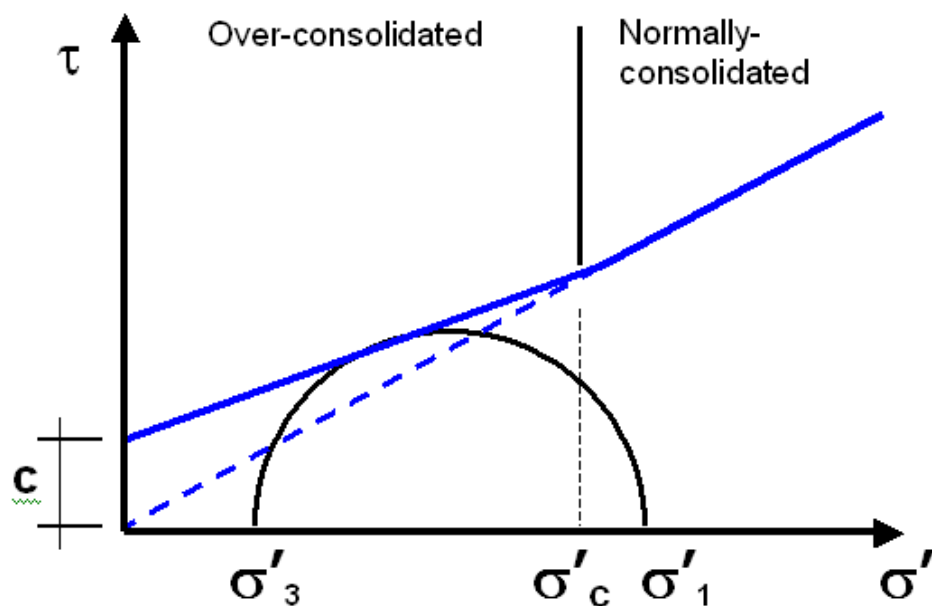


Figure 1: Transition from over-consolidated to normally consolidated failure.

Consolidated Undrained Response of Clay

The response of normally consolidated clay to loading similar to that of loose sand with a generation of positive excess pore pressures during shearing, which implies that the undrained strength is less than the drained strength.

For practical purposes, the effective friction angle ϕ' from the CU and CD tests are the same when using the conventional testing setups and speeds. For NC clays, c' is very small and is often neglected. One should however note that the undrained ‘friction’ angle from direct shear and triaxial tests are not the same.

Referring to Figure 2, suppose that we have a normally consolidated clay, which is initially consolidated to some pre-defined effective stress level. After consolidation, the state of the material is identified by point (a). When the material is sheared, the peak stress occurs when the soil reaches a second state line identified by points (b) and (d). For an undrained test, void ratio stays constant with the effective confinement decreasing, whereas during drained conditions, the confinement stays constant and the void ratio decreases; i.e., the material densifies.

When the material is over-consolidated, a unique state lines corresponding to consolidation and failure do not exist. While the tendency during shear is for the state of the material to move toward that corresponding to normally consolidated conditions, the state line is never reached. Figure 3 compares the two state lines, expressed in terms of water content, of NC and OC clay corresponding to failure.

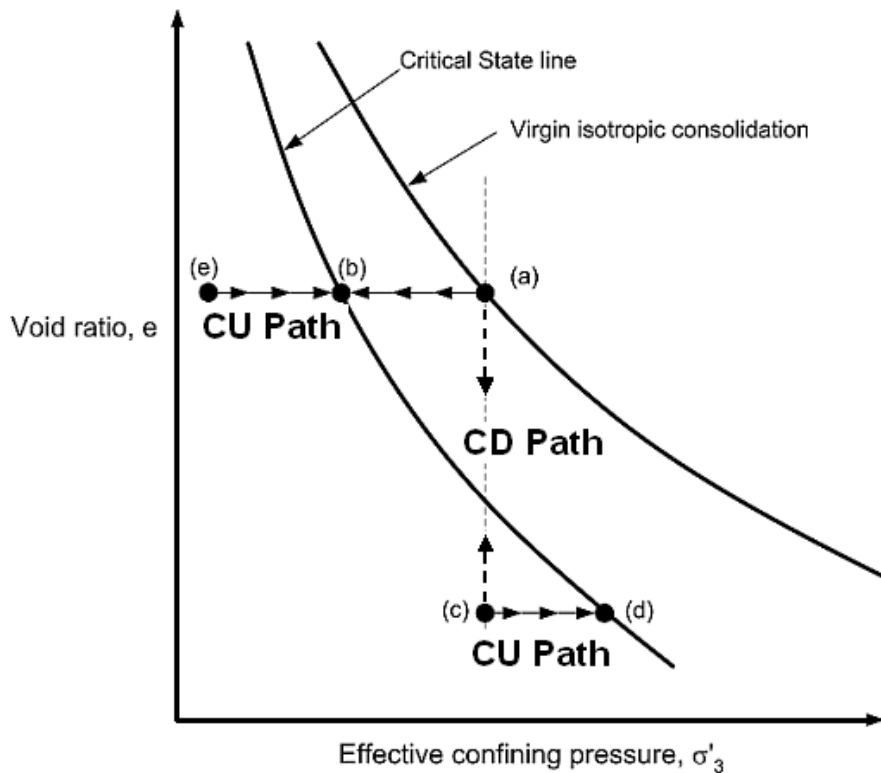


Figure 2: Changes in state during drained and undrained response of clays

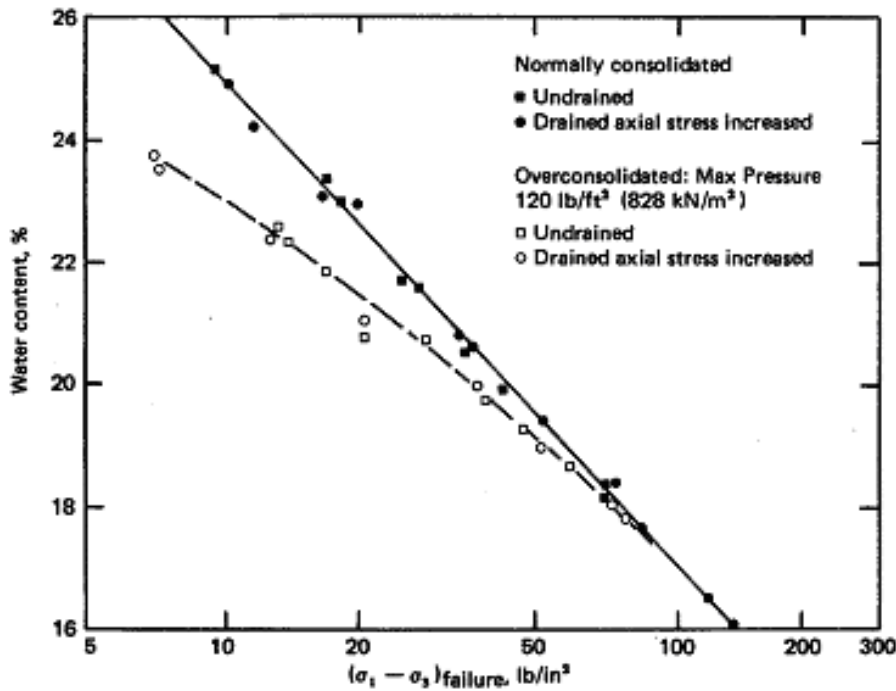


Figure 3: Figure illustrates the differences between the over-consolidated and normally consolidated states of a clay corresponding to failure.

The effective stress path for normally and over consolidated materials is illustrated in Figure 4. Although the tendencies shown are correct, a particular clay will not have the same failure envelope for NC and OC conditions.

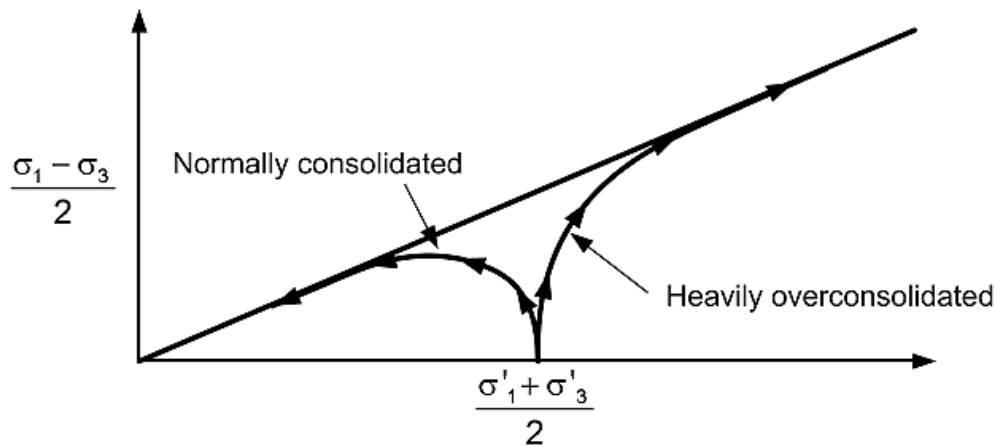


Figure 4: Undrained response of clay

Figure 5 summarizes the undrained response of NC and OC clays.

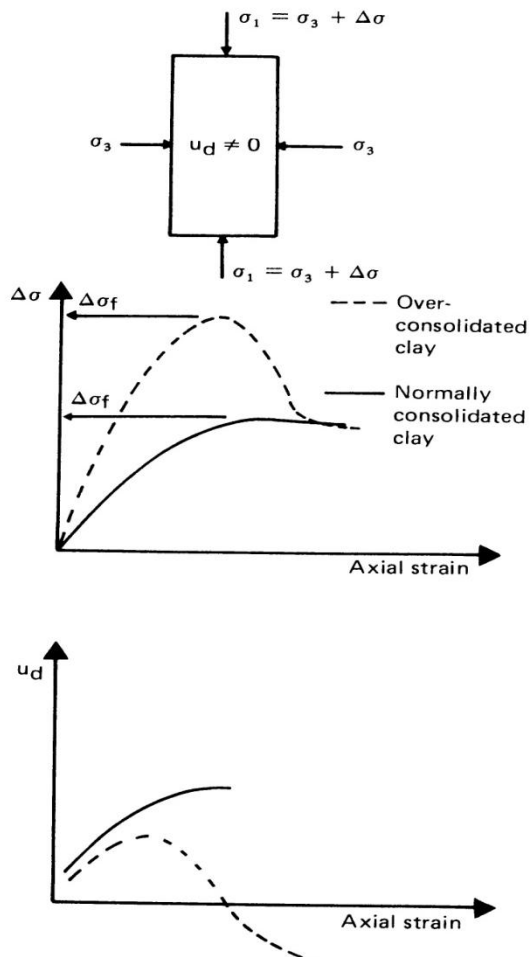


Figure 5: Summary of undrained response of clays.

Consolidated Undrained Response in Terms of Total Stresses

The failure of a soil depends on the effective stresses. Never-the-less, it is common for engineers to use failure envelopes based on total stresses, a practice that is not correct. The justification for such a practice is that pore pressures are usually not known and must be guessed in order to perform an effective stress analysis. Rather than guessing the pore pressure, the engineer prefers to deal with a known quantity. Experience has shown that, for many cases, $\tan\phi_{cu} \approx \tan\phi'/2$.

Unconsolidated Undrained Test (Strength at Constant Water Content)

For short-term stability of normally consolidated clays, total stress analysis is often used. The main difficulty with effective stress analysis is establishing the initial pore pressures as indicated above. An important assumption in the past has been that the undrained shear strength depends on water content. Therefore, shear strength can be correlated to w . Even though calculations are carried out using total stresses, the failure depends on the effective stress state as illustrated in Figure 6.

If a soil is not saturated, the UU shear strength envelope is partially curved at the beginning until all the air is dissolved in the pore water, as shown in Figure 7. For larger levels of air content, undrained conditions may not develop, since the distance to the nearest air void is close enough for Δu_w to dissipate quickly. Furthermore, for unsaturated soils one must beware of the effect of suction pressures.

For OC clays must beware of reduction in strength with time, particularly if material is unloaded. Drained long term stability controls.

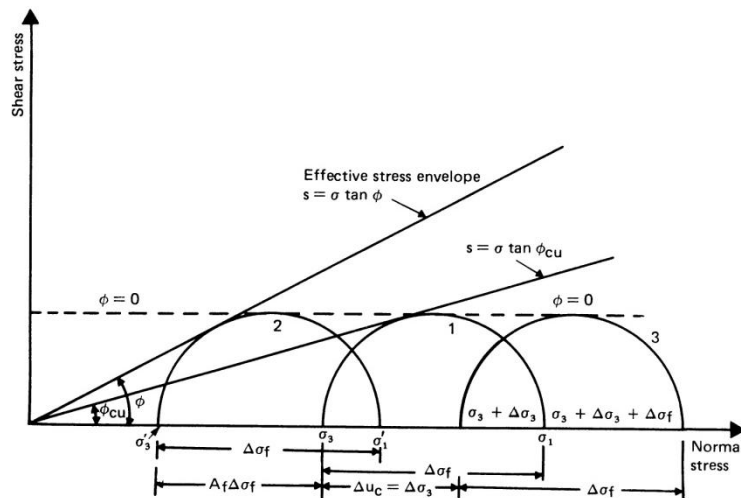


Figure 6: UU failure envelope for various confinement levels.

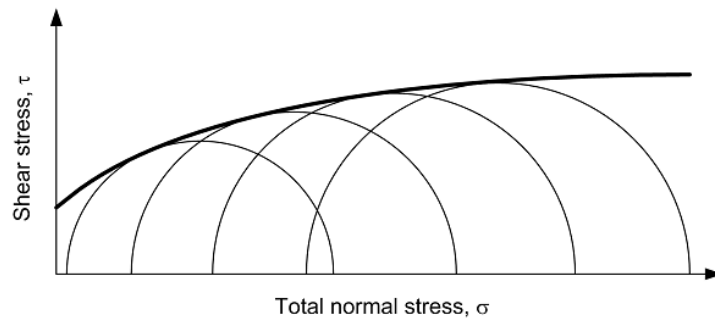


Figure 7: UU failure envelope for unsaturated soil.

Some Observations for Shear Strength of Over-consolidated Clay

For over-consolidated clay, the $e - \log \sigma'_{3f}$ relation is not the same as that for the normally consolidated clay; although at low over-consolidation ratio, the two are close. For large OCR's, say greater than 8, volume increases with shear. For small OCR's, say less than 2, volume changes are negative. In other words, the material compacts.

Figure 8 summarizes the behaviour of a cohesive soil under consolidated drained conditions. The drained shear strength of a normally-consolidated clay is higher than that corresponding to undrained conditions. The opposite is true for an over-consolidated clay.

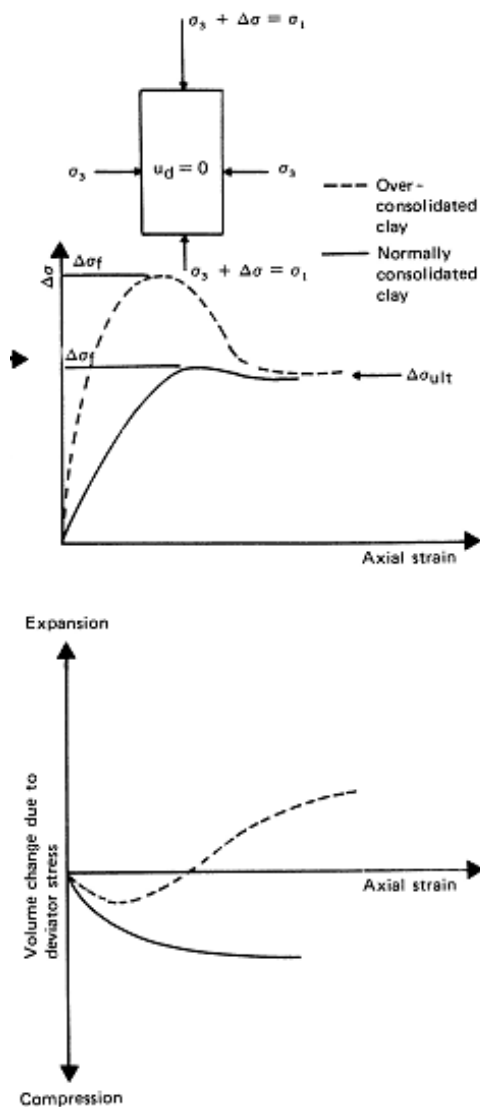


Figure 7: Summary of triaxial results of clay under CD conditions.

Sensitive Clays

Referring to Figure 8, sensitivity of a clay is defined as

$$S = \frac{q_{peak}}{q_{residual}}.$$

Some clays when sheared undergo a large change in fabric; i.e., from a flocculated structure to a dispersed structure. When this happens the sensitivity can be quite high, approaching values as high as 16. Leda clays from the Ottawa valley exhibit such characteristics. A clay is quick if $S > 50$.

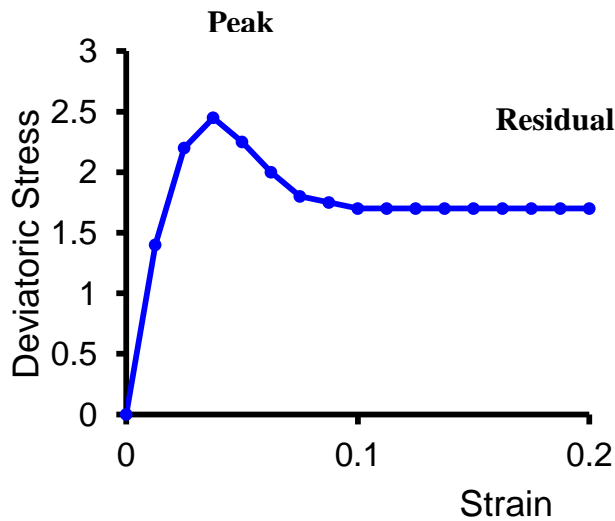


Figure 8: Definitions of peak and residual strength.

Skempton's Pore Pressure Parameters

True isotropic elastic materials do not undergo volume change when sheared. Since soils can either contract or dilate under pure shear, it is clear that they are not elastic bodies. Owing to volume change characteristics, excess pore pressures develop when a soil is sheared under undrained conditions. The amount of excess pore pressure development can be quantified using Skempton's pore pressure parameters. These parameters are useful for estimating pore *in-situ* pressure changes when changes in total stress are 2 or 3 dimensional in nature.

Without going into developmental details the increase in excess pore pressure during an undrained triaxial test is given by

$$\Delta u = B [\Delta \sigma_3 + A (\Delta \sigma_1 - \Delta \sigma_3)]$$

where $B = 1$ for soils that are saturated. The parameter A depends on stress path and deviatoric stress level relative to failure, as well as on the over-consolidation ratio, as shown in Figure 9. The main criticism of Skempton's equation is that the value of the A parameter changes as principal stresses rotate.

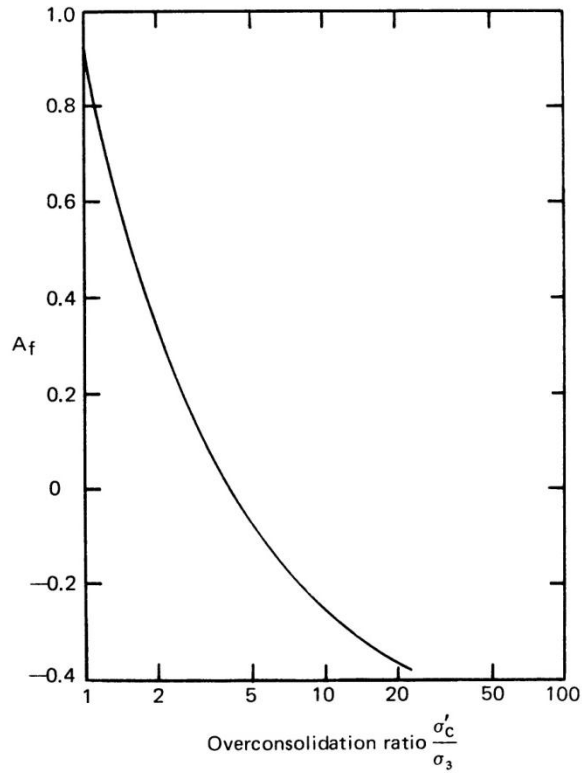


Figure 9: The sensitivity of A to over-consolidation ratio corresponding to failure.

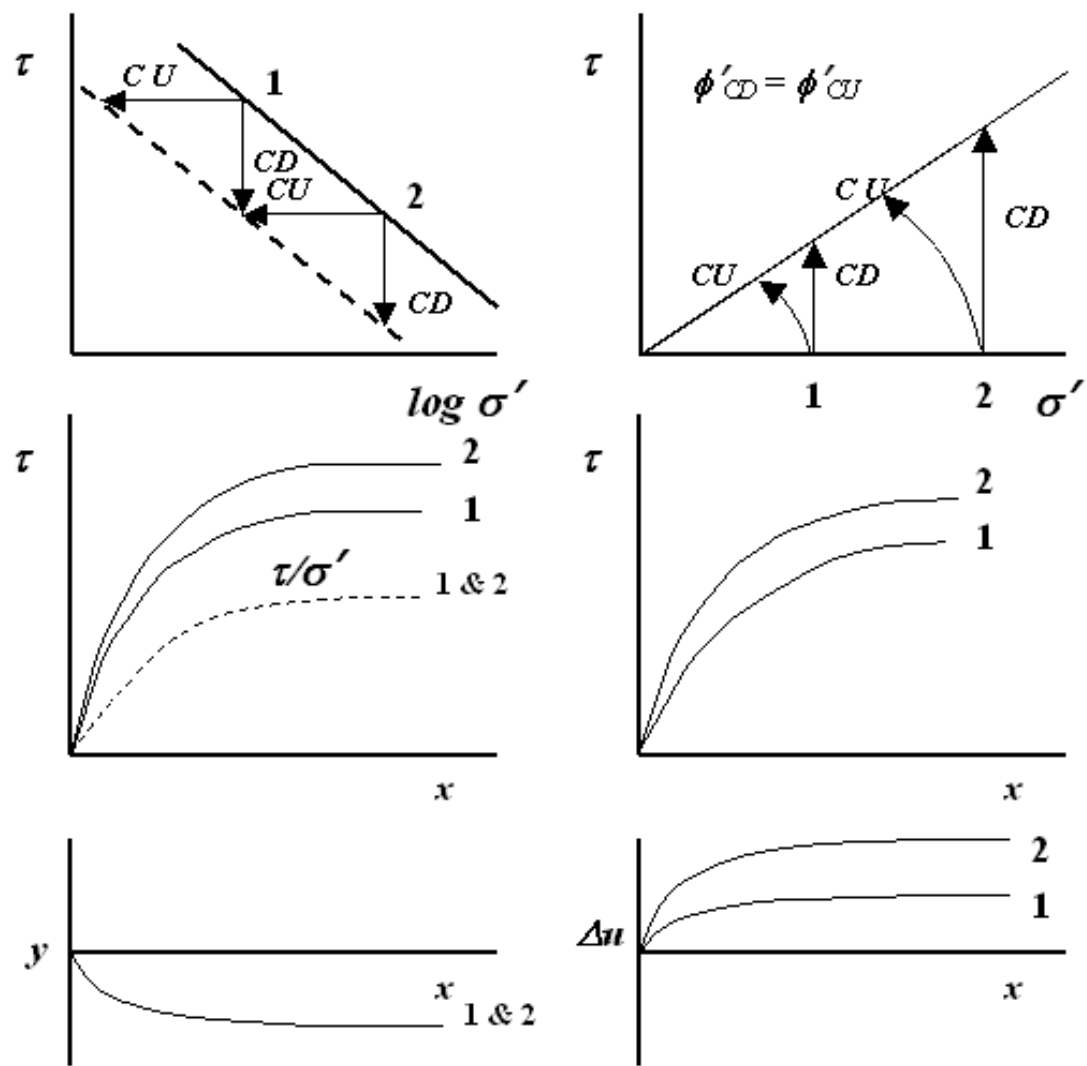


Figure 10: Summary of direct shear results for normally consolidated clay.

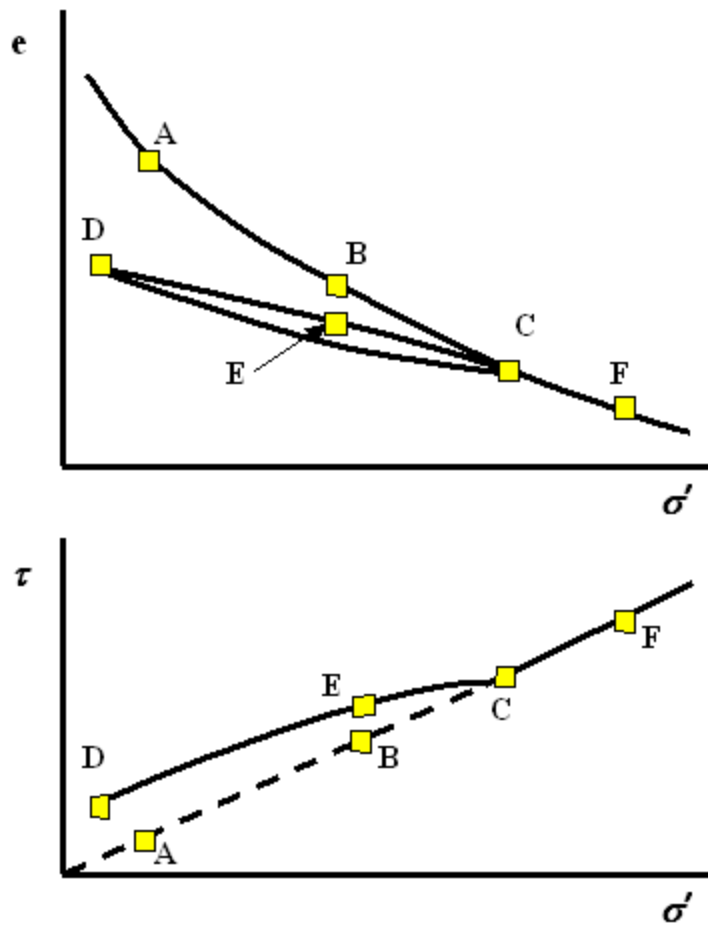


Figure 11: Summary of direct shear results for over-consolidated consolidated clay.

Retaining Walls

Introduction

Often we are encountered with the situation where insufficient room exists to permit a gradual reduction in elevation. To accommodate sharp discontinuity in elevation, we rely on retaining structures that hold back the soil mass. There are various systems for retaining soil, the choice depending on various factors including:

- Function of wall
- Soils being retained
- Availability of materials
- Labour
- Cost of construction

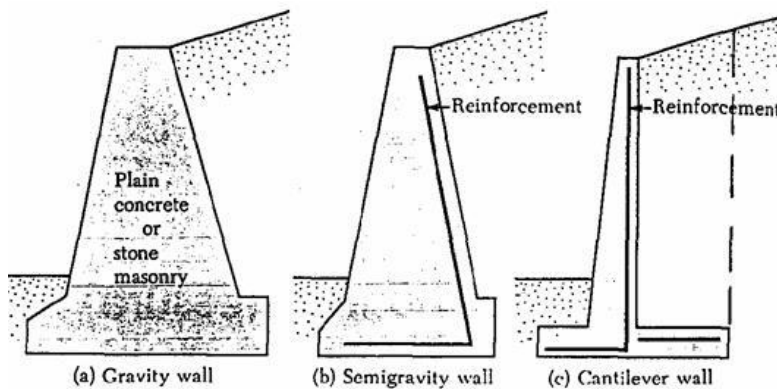


Figure 1: Typical retaining structures

In addition to those shown in Figure 1, various other retaining wall systems are presented in Figures 2 to 6. The pressures that develop behind the wall depend on the flexibility of the structure.



Figure 2: Sheet pile retaining structure



Figure 3: Rigid foundation wall construction.



Figure 4: Reinforced earth wall.

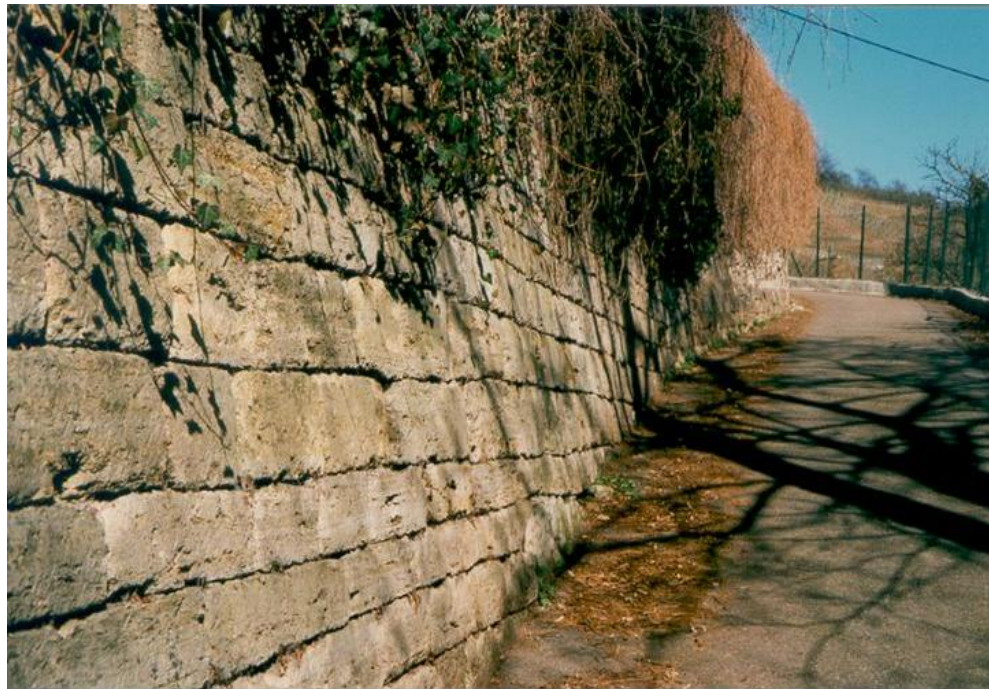


Figure 5: Dry masonry retaining wall.



Figure 6: Gabion construction.

The lateral forces that develop behind a wall are due to earth and water pressure, as well as due to structure and surface loading as illustrated in Figure 7.

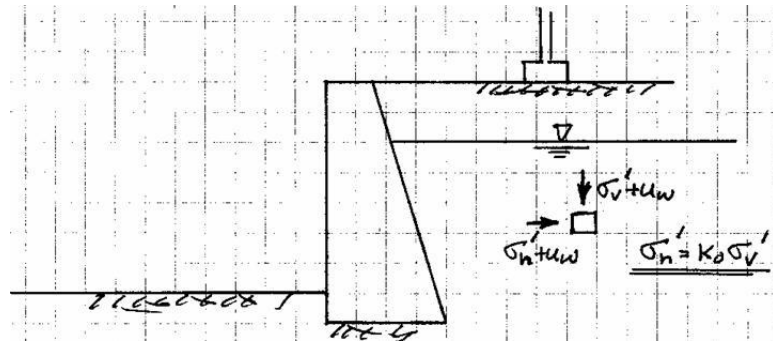


Figure 7: Factors leading to forces against retaining structures.

Lateral Earth Pressure

It is very important to recognize that the earth pressures, which develop behind and under retaining walls, are very sensitive to the amount of movement/strains that develops, see Figure 8. Since the movements/strains depend on the construction procedure, amount of compaction and flexibility of materials, they are strictly speaking unknown. The consequence is that the engineer makes use of **fictitious pressure distributions with** the accompanying analyses corresponding to limit equilibrium conditions that are conservative. If for any reason a hypothetical distribution does not yield a conservative design, the resulting forces are increased/reduced to allow for the uncertainty.

* Y = horizontal displacement and H = height of wall

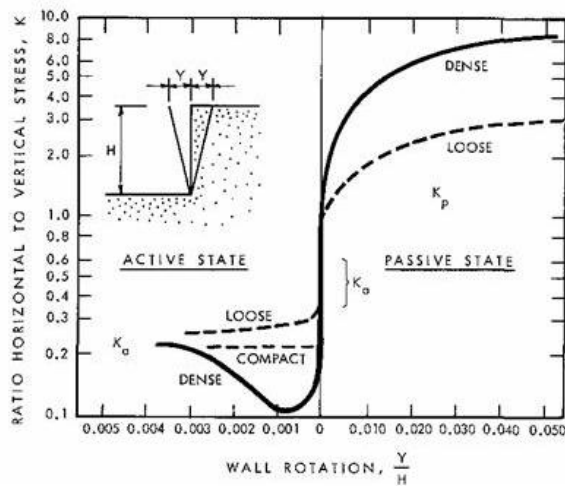


Figure 8: Significance of movement for lateral pressure development.

Earth Pressure at Rest (K_o conditions)

A situation that often arises (such as behind retaining structures acting as basement walls) is the case where we have no lateral soil movement. This situation is referred to as the K_o condition. In actual fact we always have some movement, thus the practical situation implies an apparent negligible net movement. According to the CFEM, K_o , which represents the ratio between horizontal and vertical effective stresses, may be estimated using the relation

$$K_o = (1 - \sin \phi') \sqrt{OCR} \quad (1)$$

where ϕ' is the friction angle of the soil and OCR is the over-consolidation ratio. For over-consolidated clay one can use $K_o = (0.44 + 0.42 I_p / 100) \sqrt{OCR}$.

When backfill is well/over compacted behind walls that are prevented from moving, K_o values may easily approach 1. Consequently, a value of 1 is recommended for design in such situations.

Referring to Figure 9, we see that the assumed pressure distribution against the wall is linear, and noting that it is assumed that ***no shear develops*** at the interface, the force against the wall is

$$P = \int_0^H \sigma_h dz = \frac{1}{2} K_o \gamma H^2 + \left(\frac{1}{2} \gamma_w H^2 \right) ?? \quad (2)$$

The last term on the RHS has been included to indicate that the effect of water must also be considered. For the situation shown in the figure, one should actually perform a flow net analysis and take into account the impact of water not only behind the wall, but also under and in front of the structure.

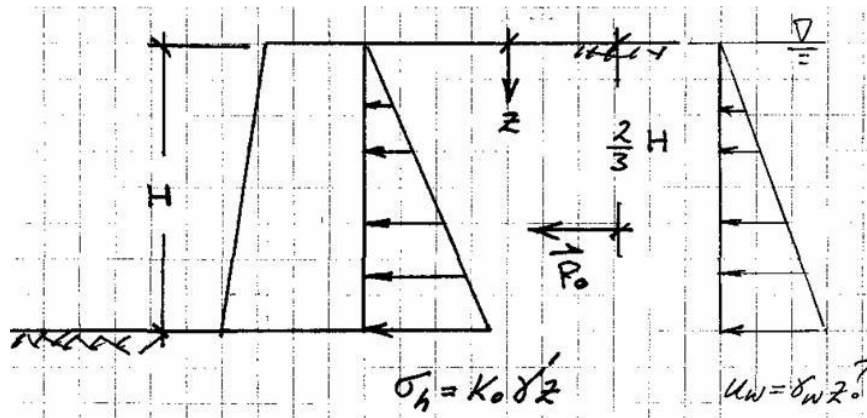


Figure 9: Assumed pressure distribution and resultant force for K_o conditions.

Active Earth Pressures

Unconstrained walls tend to move. As a result the pressures behind the wall no longer correspond to at rest conditions. There are two approaches that may be used to estimate the forces that take into account movement: **Rankine** and **Coulomb** earth pressure theories. We will begin by considering a dry cohesionless soil and Rankine theory, in which we assume: (1) horizontal surface; (2) no wall friction; (3) a wedge of soil that is in a state of limit equilibrium develops behind the wall as shown in Figure 10.

Dry Cohesionless Soil:

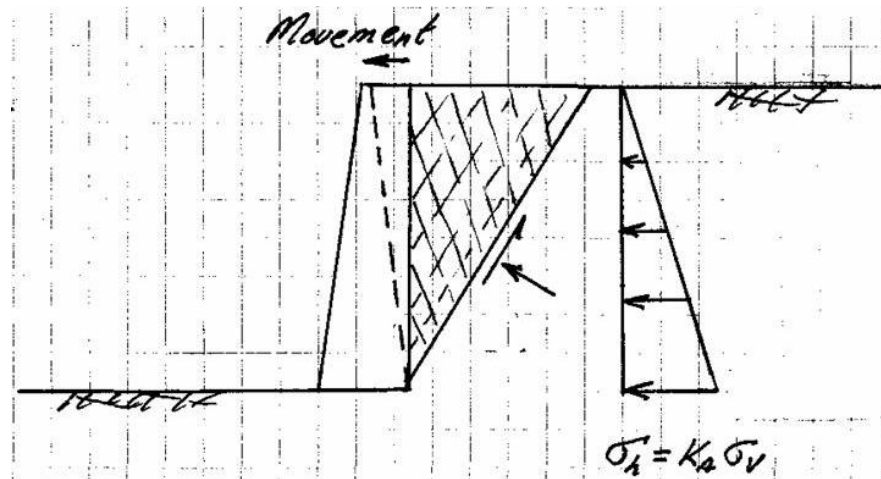


Figure 10: Development of active earth pressures.

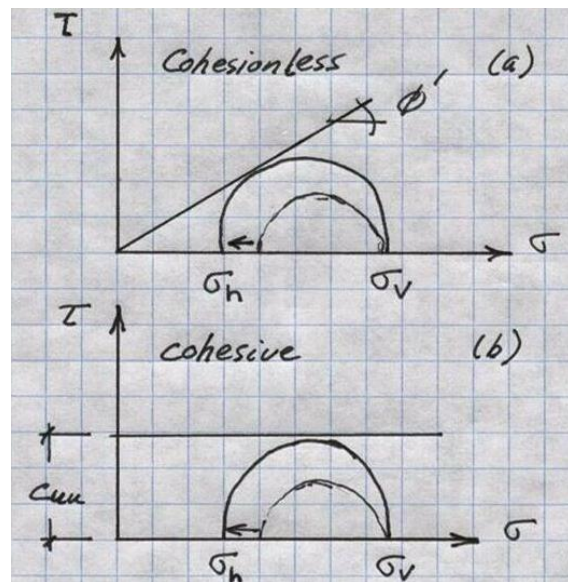


Figure 11: Limiting states of stress.

As illustrated in the figure, as the wall moves out, a zone develops in which the soil is in a plastic state of stress. The conditions for failure are dictated by the Mohr-Coulomb criterion as shown in Figure 11. It should be noted that the failure wedge is at an angle $\theta = 45^\circ + \phi'/2$ with respect to the horizontal plane. Assuming a linear distribution of vertical stress with a lateral pressure of $\sigma_h = K_a \sigma_v$, the lateral force is

$$P_a = \int_0^H \sigma_h dz = \frac{1}{2} K_a \gamma H^2 \quad (3)$$

with

$$K_a = \frac{1 - \sin \phi'}{1 + \sin \phi'} = \tan^2(45 - \phi'/2) \quad (4)$$

The key here is developing sufficient movement; see Figure 10. Given the shape and orientation of the wedge, the wall need only rotate about the toe of the base.

Cohesive Soil:

Although it is highly undesirable to place cohesive soils behind retaining structures, at times it is unavoidable. Usually, the analyses are carried out in terms of total stresses together with UU test parameters. Referring to Figure 11, the limiting horizontal pressure is

$$\sigma_h = \frac{\sigma_v - 2c}{\gamma z - 2c} \quad (5)$$

where c is the cohesion from the UU test, with the subscripts dropped for convenience. Unlike cohesionless soils, cohesive soils can support short term tension due to soil suction. Figure 12, illustrates the variation in pressure.

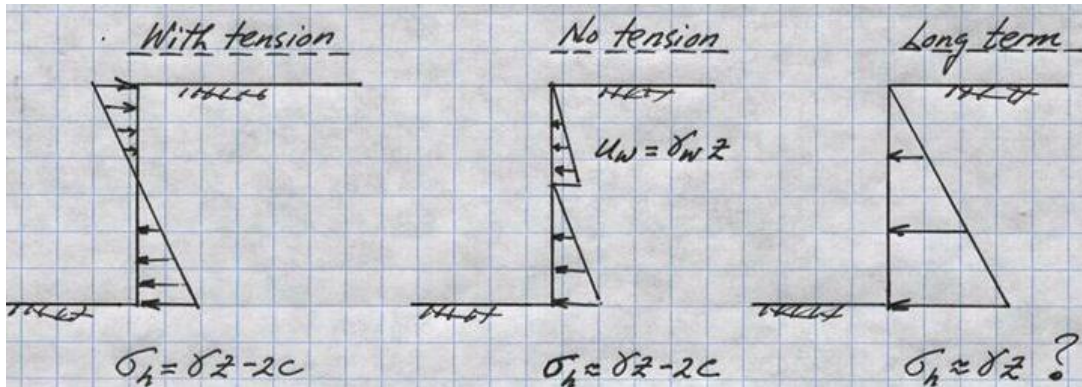


Figure 12: Variation of cohesive soil pressure behind retaining wall.

Unfortunately, the suction is not reliable, and cracks can develop and fill with water. The depth to which cracks extend is approximately by

$$z_c = \frac{2c}{\gamma} \quad (6)$$

For short-term situations, the net force on a retaining structure with full soil suction could be as low as

$$P_a = \frac{1}{2}\gamma H^2 - 2cH \quad (7)$$

Using this equation, an unsupported vertical slope may remain stable to a height

$$H_c = \frac{4c}{\gamma} \quad (8)$$

that is, the height at which a wall would have no net force. One must exercise extreme caution when applying this equation. For practical designs, supports are specified for $H > H_c/2$ in case of tension cracks developing.

It must be stressed that the undrained, total stress, stability analysis is only for the short term since soft soils often creep leading to redistribution of pressure and an increase in lateral pressure. Besides, a redistribution of pore pressure and water content occurs over time, thus leading to changes in soil strength.

Passive Earth Pressures

If a wall moves into a soil rather than away, passive pressures are developed that greatly exceed those corresponding to K_o conditions. The reason for this is that horizontal stress is no longer the minor principal stress, but rather the major principal stress. The corresponding pressure distributions are given by

$$\begin{array}{ll} \text{cohesionless} \Rightarrow & \sigma_h = \frac{K_p \sigma_v}{\gamma z + 2c} \\ \text{cohesive} \Rightarrow & \end{array} \quad (9)$$

where $K_p = 1/K_a$.

A common situation where passive stresses are developed is in front of a retaining wall and shown in Figure 10. Given that much larger displacements are required to develop passive pressures when compared with active ones (see Figure 9), and the availability of the reaction may be questioned at times (erosion, excavation, etc.), an additional factor of safety is often imposed on the passive reaction to take into account the uncertainty.

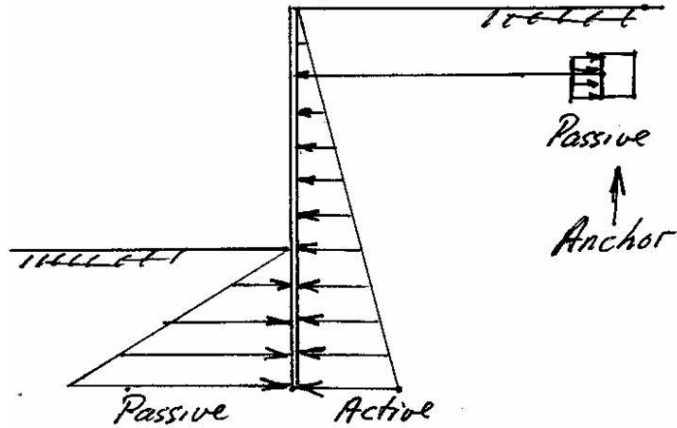


Figure 13: Development of passive pressures for sheet pile wall construction.

Coulomb Earth Pressure Theory

Coulomb's procedure considers force equilibrium without regard to the pressure distribution, although most often we assume that the variation is linear. This theory easily accommodates wall friction and slopes that are not horizontal, as well as concentrated loads. Referring to Figure 14, one assumes a distinct failure plane develops and that the wedge itself is rigid. By assuming a limiting stability condition along the failure plane as well as at the wall-soil interface, one can determine the force P required to maintain overall equilibrium for a given θ . The objective is to find the force P_a that maximizes P . For the passive case, we search the force P_p that minimizes P . One must be aware that the direction of the forces must be consistent with the failure mechanism.

Note:

- For the Rankine situation, the Coulomb procedure yields identical results. It should be noted that the Rankine theory tends to overestimate active forces and underestimates the passive ones.
- Wall friction δ can vary between 0 and ϕ' . The rule of thumb is

Smooth concrete wall	$\frac{\phi'}{2} < \delta < \frac{2}{3}\phi'$
Rough concrete finish	$\delta \approx \phi'$

- Wall friction has the tendency to reduce the active force on the wall.

- If $\delta > \phi'/3$, Coulomb's theory can greatly overestimate the passive force as the failure surface begins to greatly deviate from a plane.
- If the flexibility of the wall and resulting movement is vastly different from that assumed, the magnitude and direction of the earth pressure change. This is particularly true for flexible, sheet pile walls and braced excavations.

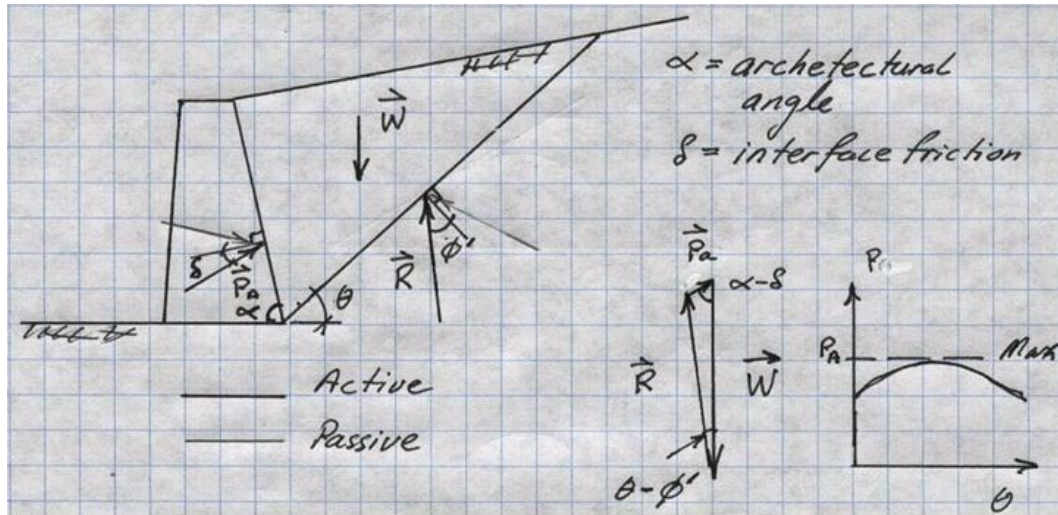


Figure 14: Free-body diagram for Coulomb analysis.

Stability Considerations

Again, sufficient wall movement is required to get the forces right.

- **Basal Sliding Stability** – Referring to Figure 15, the factor of safety with regard to sliding is

$$F_s = \frac{T + P_p}{P_h} \geq 2 \quad \text{or} \quad F_s = \frac{T}{P_h} \geq 1.5$$

If water pressure develops behind and in front of the wall, this must also be taken into account. Some suggest using a factor of safety of 1.5 for granular backfill and a value of 2.0 for cohesive backfill. Common values for the coefficient of friction at the base are given by

$$\tan \phi' > \mu > \frac{2}{3} \tan \phi'$$

$$0.5c \leq c_b \leq 0.75c$$

- **Overshooting Stability about Toe** – $F_s = \frac{Wd}{P_a a}$

This expression compares the stabilizing moments to the overturning moments. Suggested factor of safety is 1.5 for granular backfill and a value of 2.0 for cohesive backfill.

- **Allowable Bearing Capacity** – In order to ensure stability of the base, the resultant force acting at the base must pass through the middle third of the footing; i.e., $B/3 < d < 2B/3$. Taking into account depth factors as well as load inclination factors, the bearing capacity q_u is calculated using the footing equations. The allowable pressure q_a is estimated as

$$\frac{q_u}{4} \leq q_a \leq \frac{q_u}{3}$$

with

$$q_{\max} = \frac{N}{B} \left(1 + \frac{6e}{B} \right) \leq q_a$$

where q_{\max} is the maximum pressure assuming a linearly varying pressure distribution under a base of unit length.

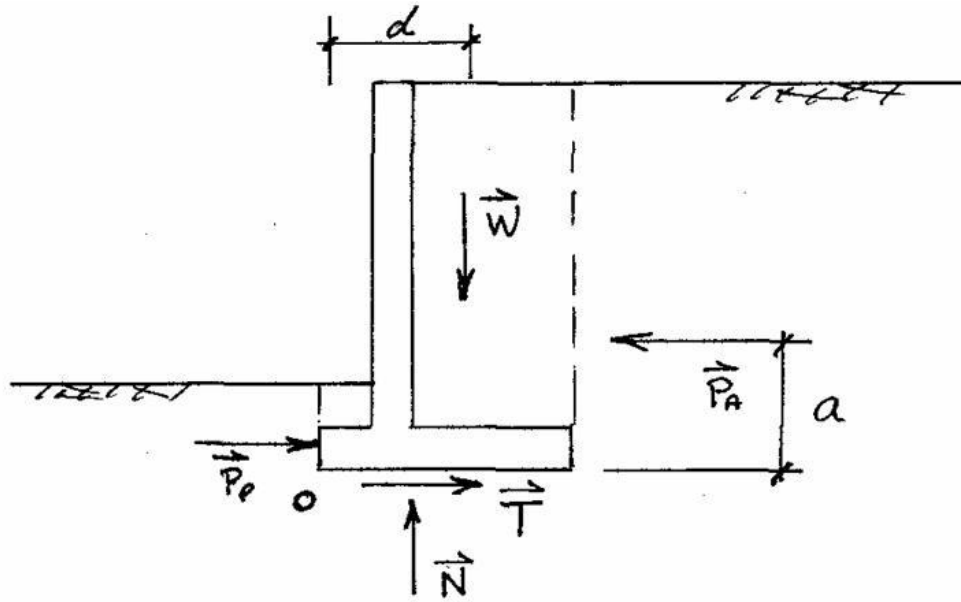


Figure 15: Forces acting on cantilever wall.

Sample Problem

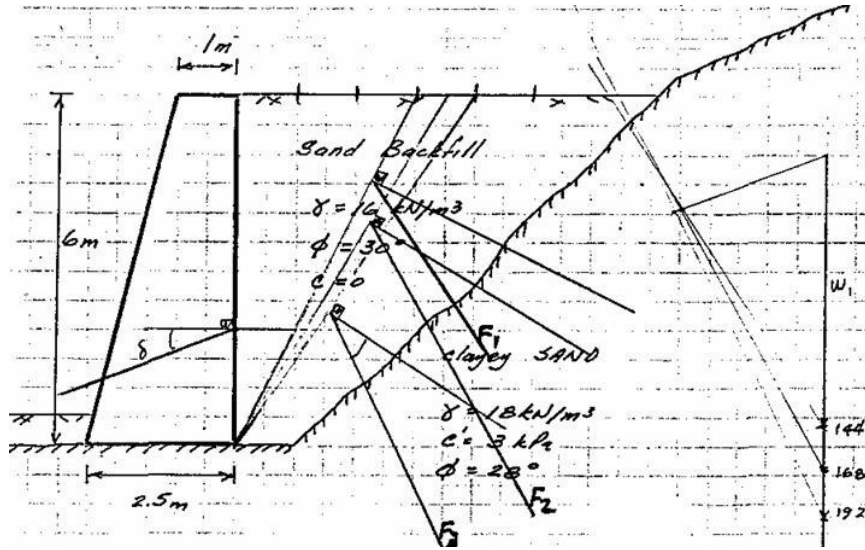


Figure 16: Sample problem for gravity wall.

Drainage

For adequate long term performance of a retaining wall, adequate drainage is required behind the wall. Most often this consists of a cohesionless drainage layer immediately adjacent to the wall. While the assumption is that this layer allows for rapid drainage, the layer may actually act as a barrier if it separates the wall from a fine-grained soil. This is due to the fine-grained soil having a ‘higher’ hydraulic conductivity than an unsaturated coarse-grained soil. The conductivity however increases substantially as the degree of saturation of the drainage layer increases.

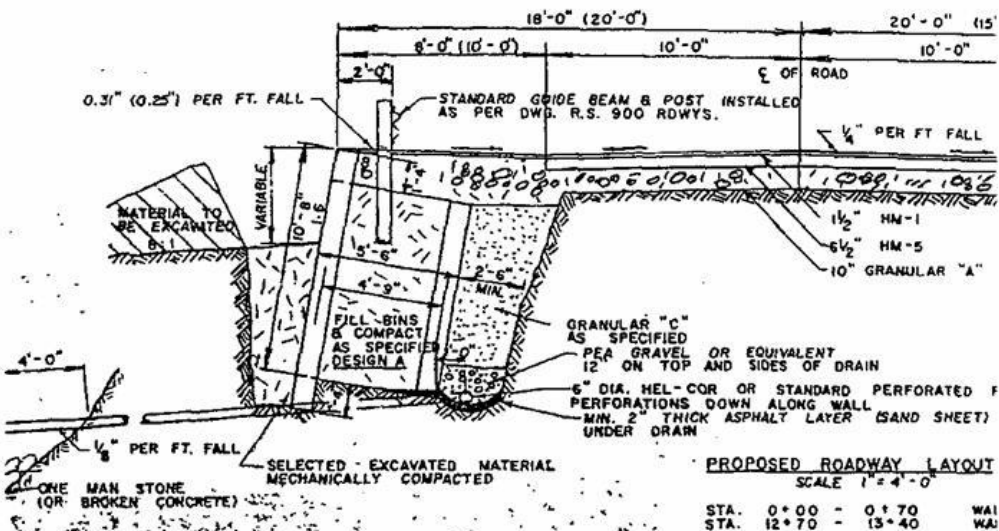


Figure 23: Drainage provisions behind retaining wall.

Bearing Capacity (Shallow Foundations)

Introduction

A foundation transfers the load of the superstructure to the underlying soil/rock formation without overstressing any of the components. In addition to stability considerations, the design bearing pressure is limited by the allowable post-construction settlement. The ultimate q_u and allowable q_a bearing capacities of the soil are related to one another through the relation $FS = q_u/q_a$. Foundations must be placed deep enough to ensure that their performance is not affected by seasonal changes, including frost heave, volume changes due to moisture changes and scour.

By definition, a shallow foundation, which refers to the structural element, is often defined as one, which has a width greater than the depth at which it is placed; i.e. $D_f/B \leq 1$.

Considerations include:

- Action and magnitude of applied load
- Structural capacity of the foundation and properties of the underlying soil
- Surrounding topography and location of adjacent structures
- Quality and quantity of materials
- Constructability
- Unexpected site conditions
- Minimization of labour and cost

The distribution of pressure and stress under foundation is sensitive to:

- Magnitude of applied load
- Distribution of properties and regolith layering
- Its flexibility relative to that of the underlying medium
- Dimension of foundation relative to layer thicknesses

While the distribution of pressure can be quite complex, it is usually assumed to be uniform.

Types of Footings

- Strip/wall – Long, narrow footing (see Figures 1 and 2)
- Spread (rectangular/circular) – Column tends to be located at centroid of section
- Combined – One or more columns supported by one foundation (see Figure 3)
- Strap – Two spread footings joined with strap for shear transfer
- Mat – Footing over entire building area, carrying walls and columns; recommended if at least half of building area covered by footings; can bridge soft material



Figure 1: Forming of strip footing to support wall.



Figure 2: Reinforcing steel in strip footing.



Figure 3: Combined footing that supports bridge piers.

Estimates of Allowable Bearing Pressure

The allowable pressure can be obtained by carrying out an engineering analysis using measured soil properties. On the other hand, a wealth of experience provides us with estimates that may be used for preliminary design.

Failure Patterns

Models of footings on sand have identified three stages during loading:

1. Soil beneath the footing is initially forced downward to form a rigid cone (wedge), with the soil outside the wedge being forced up; and
2. Soil around the foundation perimeter pulls away from the footing and surfaces of shear propagate outward from the tip of the cone.

For a soil that is compressible or ductile **local shear failure** occurs in which failure is progressive and confined to fan-shaped shear zones ($A'CB$ and ABC' in Figure 4). Rigid soils tend to undergo **general shear failure** in which the failure surface propagates to the ground surface, assuming $D_f = 0$ ($A'DCB$ and $ABC'D'$). **Punching shear failure** involving little horizontal strain around the periphery of the footing and thus no or little bulging occurs for loose and very soft soils. For cohesionless materials, the type of failure depends on the soils relative density and depth of burial.

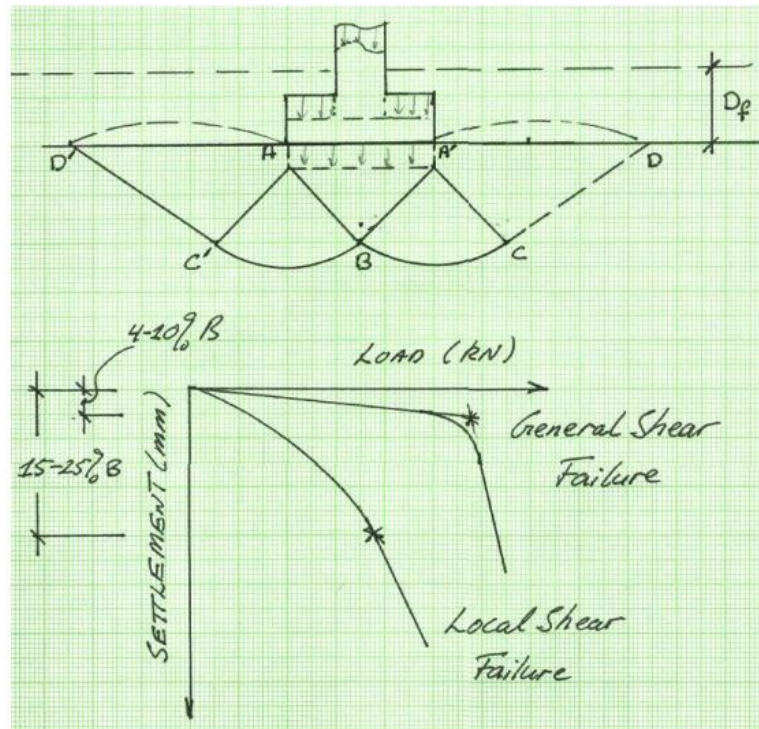


Figure 4: Failure pattern for shear failure and corresponding load-settlement curves.

There is no exact mathematical analysis for bearing capacity failure. The approximations that have been developed assume general shear failure. To take into account that a footing is below the ground surface, the effects of the soil are introduced as a surcharge, whose shear resistance is neglected. Before going on to the more popular theories, bearing capacity based on Rankine wedge approximation is considered.

Bearing Capacity Via Rankine Wedges

Referring to Figure 5, we have a strip footing of width B and infinite length supported by a cohesionless material. The bottom of the footing is located a distance D_f below the ground surface and the water table is well below the zone under consideration.

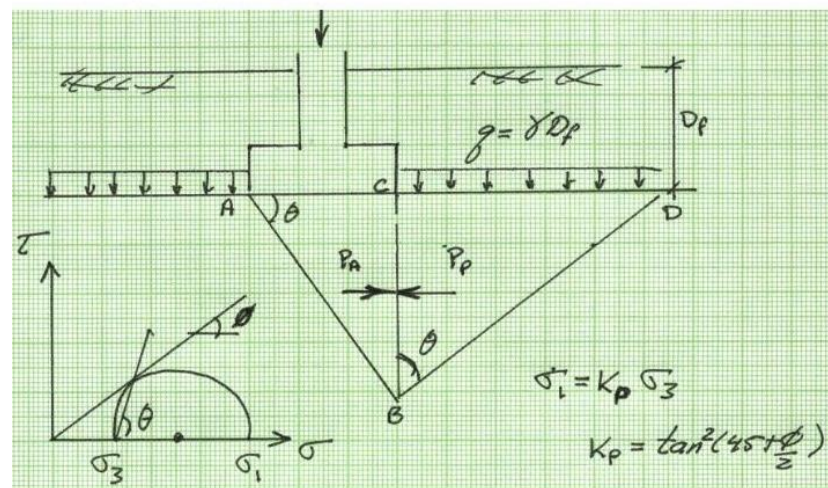


Figure 5: System of forces assuming Rankine wedge failure mechanism

The following is assumed:

- The bottom of footing is frictionless with zone ABC in an active state of stress.

$$\sigma_h = K_a (\gamma z + q_u) \quad \text{and} \quad P_a = \int_0^H \sigma_h dz$$

where q_u is the ultimate bearing capacity and $H = B \tan(45 + \phi/2)$ is distance BC and B is the width of the footing.

- The region CBD is in a passive state of stress

$$\sigma_h = K_p (\gamma z + \gamma D_f) \quad \text{and} \quad P_p = \int_0^H \sigma_h dz$$

- Shear stresses along BC are neglected, thus the net force for each wedge acts horizontally. By observing that the force from both wedges must be the same for equilibrium; that is, $P_a = P_p$, one has

$$q_u = qN_q + \frac{1}{2}\gamma BN_\gamma$$

with bearing capacity factors $N_\gamma = K_p^{2.5} - K_p^{0.5}$ and $N_q = K_p^2$.

A similar analysis can be completed for a cohesive soil for which total stresses are considered such that $\phi_u = 0$ and failure is defined by $\sigma_1 = \sigma_3 + 2c_{uu}$, in which c_{uu} is the cohesion. It is possible to show that

$$q_u = 4c_u + q$$

where q is the surcharge associated with embedment. Given that the unit weight of the footing is similar to that of the soil, often engineers deal with the ***net ultimate bearing capacity***

$$q_{unet} = q_u - q = 4c_u$$

The justification for using this form is that the soil is already supporting a stress level q , and the factor of safety should be applied to the loading that is over and above the existing equilibrium state.

General Bearing Capacity Equation

Although there are several bearing capacity equations, the one proposed by Terzaghi is still often preferred by practicing engineers. While the failure mechanism is different from that of the previous section, the analysis contains similar elements. An important difference is that it friction does develop between the footing and soil, forms a cone that remains elastic with $\theta = \phi$. With reference to Figure 1, the fan is referred to as the zone of radial shear. Assuming once again a strip footing, we have for a concentrically loaded footing

$$q_u = cN_c + qN_q + \frac{1}{2}\gamma BN_\gamma$$

where N_c is the third bearing capacity factor related to the cohesion term. For the case of local shear failure Terzaghi proposed that c be replaced by 0.67 c and $\tan\phi$ by 0.67 $\tan\phi$. The values of the bearing capacity factors are functions of the friction angle. Strictly

speaking, these factors must be modified to take into account variables such as footing shape, depth, load inclination and proximity to a slope.

Although several similar equations have been proposed, Terzaghi's equation is the easiest to use and practitioners often question the effort going into taking into account the other factors when at the end of the calculations the ultimate value is factored by an arbitrary factor of safety that has been likely calibrated using the Terzaghi approach. Nevertheless, the Canadian Foundation Engineering Manual (CFEM) proposes the use of Brinch-Hansen coefficients

$$\begin{aligned} N_q &= e^{\pi \tan \phi} \tan^2(45 + \phi/2) \\ N_c &= (N_q - 1) \cot \phi && \text{for } \phi = 0 \quad N_c = 5.14 \\ N_\gamma &= 1.5(N_q - 1) \tan \phi \end{aligned}$$

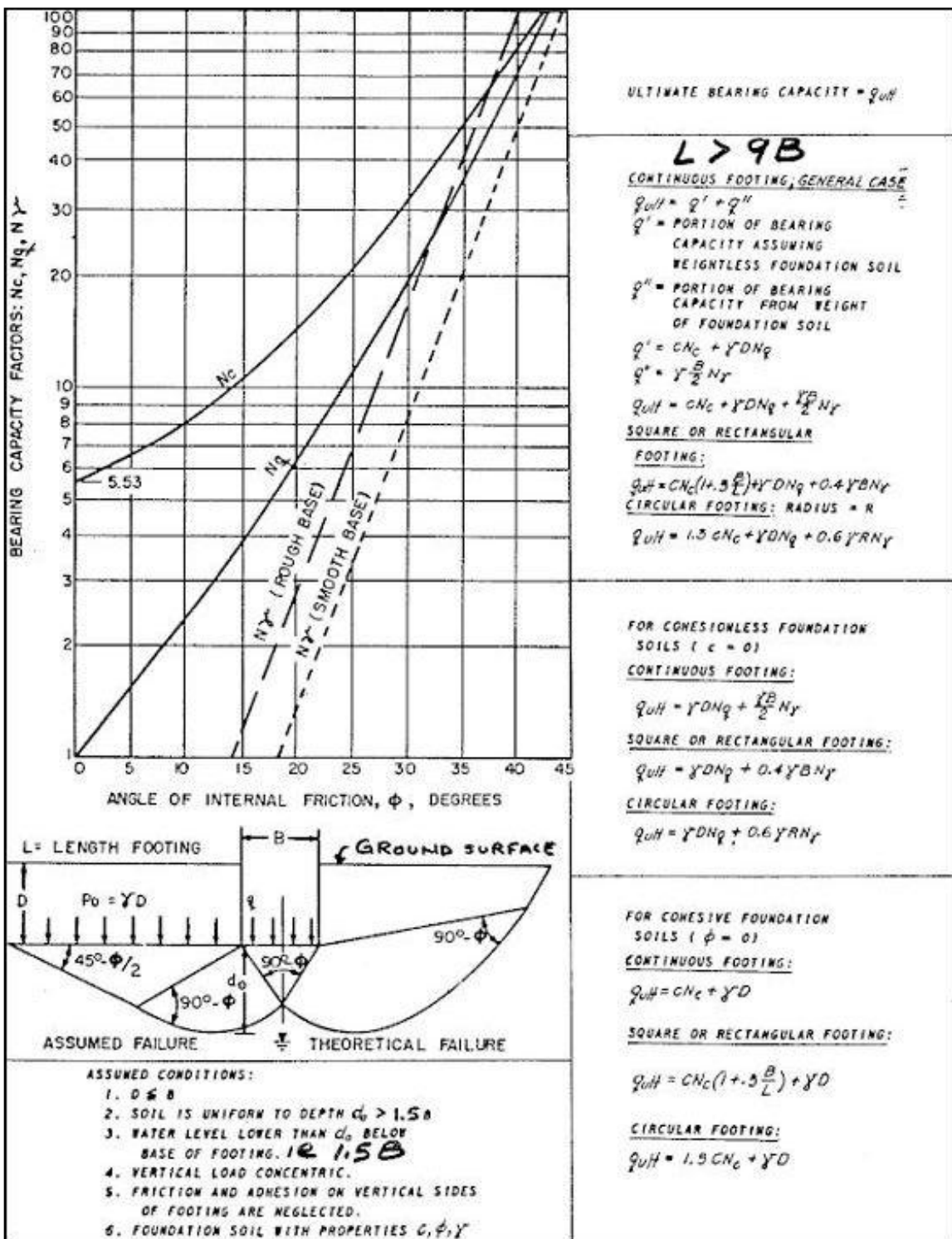
Owing to the sensitivity of the coefficients to ϕ , especially for values above 30° , considerable judgment must be used. One must remember that the properties that are of interest are those within a depth of $1.5B$. Properties should be sampled to a depth of at least $2B$.

Note: $Q_u = BL q_u$ usually depends on the strength of the soil within $1.5B$, but one should have SPT indices up to $2B$.

Since Terzaghi's equation applies to a strip footing subjected to vertical loading, the bearing capacity coefficients must be modified using

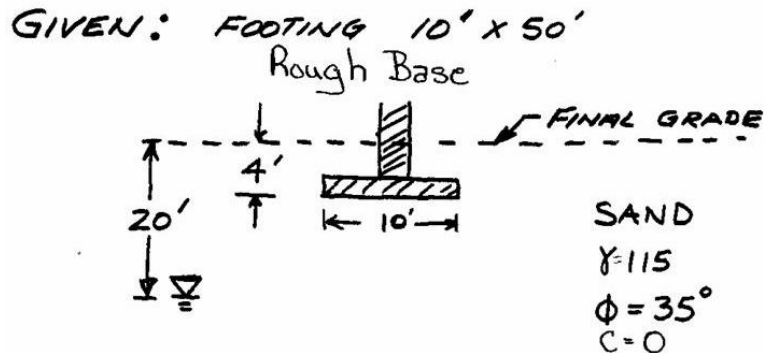
$$\begin{array}{lll} s_q = 1 + \left(\frac{B}{L} \right) \left(\frac{N_q}{N_c} \right) & & i_q = \left(1 - \frac{\delta}{90^\circ} \right)^2 \\ \text{Shape Factors:} \quad s_c = 1 + \left(\frac{B}{L} \right) \left(\frac{N_q}{N_c} \right); & \text{Inclination Factors:} \quad i_c = \left(1 - \frac{\delta}{90^\circ} \right)^2 \\ s_\gamma = 1 - 0.4 \left(\frac{B}{L} \right) & & i_\gamma = \left(1 - \frac{\delta}{\phi} \right)^2 \end{array}$$

where δ is the inclination of the load relative to the vertical direction.



Bearing Capacity Factors from NAVFAC

Problem (Cheney and Chassie, Soils and Foundations Workshop Manual, US Department of Transportation, 1982)



**FIND: ALLOWABLE BEARING CAPACITY
FOR SAFETY FACTOR = 3**

Eccentrically Loaded Footing

The pressure distribution under a footing is quite complex. The complexity increases if the loading is eccentric. Referring to Figure 6 where we have one way eccentricity, it is assumed that the pressure varies linearly such that for a footing of length L and width B to simplify the analysis

$$\frac{q_{\min}}{q_{\max}} = \frac{Q}{BL} \mp \frac{6M}{B^2 L} \quad \text{or} \quad \frac{q_{\min}}{q_{\max}} = \frac{Q}{BL} \left(1 \mp \frac{6e}{B} \right)$$

in which e is the eccentricity. For the case where $e > B/6$, the analysis predicts that q_{\min} goes into tension, which is undesirable. Consequently, the design should ensure that the resultant load falls within the middle third; i.e., $e < B/6$. As a point of reference, for $e = B/6$, $q_{\max}/q = 2$ with $q = Q/BL$. This means that if a footing is designed for a factor of safety of 2 neglecting eccentricity then the edge of the footing is at ultimate conditions.

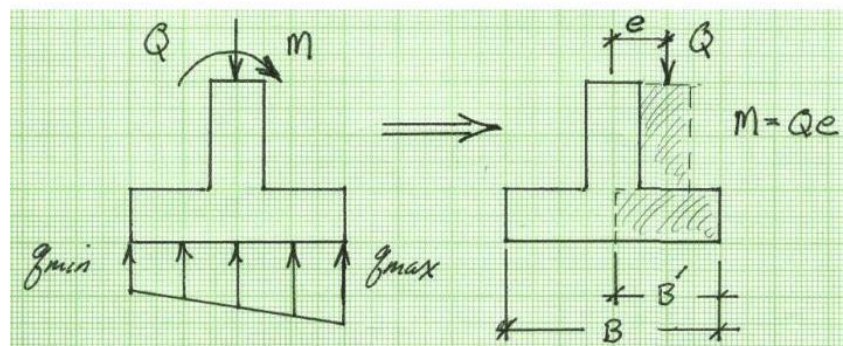


Figure 6: Eccentrically loaded footing and equivalent width $B' = B - 2e$.

To accommodate eccentricity, Meyerhof suggested using an equivalent footing of width $B' = B - 2e$ when applying the bearing capacity equations. By using the effective width, the load is assumed to be applied at the centroid of the effective footing as shown in Figure 6. the load per unit length supported by the hypothetical footing is $Q_u = Bq_u$.

When reviewing the literature, it appears that the Meyerhof approach is recommended primarily for the case $e > B/6$. From a practical point of view, one could also specify the requirement $q_{average} < q_a$ and $q_{max} < 1.3 \cdot q_{average}$. One must remember that the analyses are not exact.

Effective Stress versus Total Stress Analysis

By and large, the bearing capacity equations apply to an effective stress analysis. As a result it is necessary to consider the influence of the groundwater table. Given that D_w is the depth of the GWT below the footing, no adjustments are required if $D_w > B$. On the other hand if $D_w/B < 1$, an equivalent unit weight $\gamma_e = \gamma_b(1 + D_f/B)$ is required for the term associate with N_γ . For the GWT above the bottom of the footing then one must use for the N_q term the effective surcharge q' , which takes into account the buoyant unit weight γ_b of that part of the soil that is saturated.

The most notable exception to effective stress analysis is the situation where short term stability controls the design and total stresses are used together with the $\phi_{uu} = 0$ analysis. According to Skempton (1951), for a clay with $D_f/B < 2$

$$q_u = 5c_{uu} \left(1 + 0.2 \frac{B}{L} \right) \left(1 + 0.2 \frac{D_f}{B} \right) + q .$$

When using this equation, it is not uncommon to express the factor of safety in terms of the net ultimate strength; i.e., $FS = q_{unet}/q_{anet}$.

Example – Consider a truck supported by a soft clay where $c_{uu} = 50$ kPa. The bearing capacity is estimated as $q_u = 5(50) = 250$ kPa. Truck tires are often inflated to 550 kPa pressure. As one can tell, the clay cannot support the truck.

Note: For many situations the soil is partially saturated and the clay/silt may be subjected to large suction pressures. This possibility must be taken into account as changes in water content could lead to large changes in undrained shear strength.

Settlement Calculations

In many, if not most situations, the footing size is controlled by settlement considerations. While simple relations exist for calculating the settlement under a footing associated with

an elastic half space, most real problems are much too complex to be accurately described. As a result, approximate techniques involving estimates of stress increases and soil compressibility are often adopted, at least for preliminary design.

The settlement calculation assuming that one-dimensional vertical compression dominates, involves:

- estimating the average effective stress increase $\Delta\sigma'_v$ in layer i
- determining the average strain $\varepsilon_i = \Delta\sigma'_v/E$
- calculating the change in layer thickness $\Delta H_i = \varepsilon_i H$
- summing up the contributions from each layer $\Delta H = \sum \Delta H_i$

Estimating Stress Increase – The starting point for most analyses is the elastic solution by Boussinesq equation for a point load P applied at the surface:

$$\Delta\sigma_v = \frac{3P}{2\pi} \frac{z^3}{(\sqrt{r^2 + z^2})^5}$$

where r is the offset from the load and z the depth below the surface. An examination of this equation reveals that it does not require material properties. It has been convoluted to provide solutions for various distributions of surface load.

Given that the distribution of stress under a footing is not well defined, an alternative approximation based on the 2:1 rule is often adopted for finding the increase in stress along the centerline. Referring to Figure 7,

$$\Delta\sigma_v = \frac{P}{(B+z)(L+z)}.$$

Strain Calculation – The compressive straining of the soil depends very much on the rate at which excess pore pressure can be forced out of the voids. For cohesive soils, the settlements are dominated by the time-dependent volume changes. Assuming a normally-consolidated fine-grained material, we may write for the maximum strain

$$\varepsilon = -\frac{\Delta e}{1+e_o} = C_c \log_{10} \left(\frac{\sigma_o + \Delta\sigma'_v}{\sigma_o} \right).$$

in which e is the void ratio and the other terms take on their usual definitions. The compression index can be estimated using the natural water content w : $C_c \approx w/100$, with the recompression index for over-consolidated soil $C_r \approx w/1000$.

Total Settlement - The settlement under the structure is obtained via $\Delta H = \sum \varepsilon_i H_i$. If consolidation is important, then the settlement develops over time t such that

$\Delta H(t) = U(T)\Delta H$ in which U is the degree of consolidation that depends on the time factor $T = c_v t / H_d^2$ with c_v being the coefficient of consolidation and H_d the drainage path.

For some soft soils it is also necessary to consider **secondary settlement** due to the creep of the soil skeleton; i.e., $\Delta H_{ss} = C_\alpha H \log_{10}((t - t_p)/t_p)$ in which C_α is the coefficient of secondary consolidation and t_p refers to the time for primary consolidation.

Settlements are usually overestimated, given: structural load causing settlement is often overestimated; construction settlements are not taken into account; pre-consolidation is not properly taken into account; and 3-D influences are not properly identified.

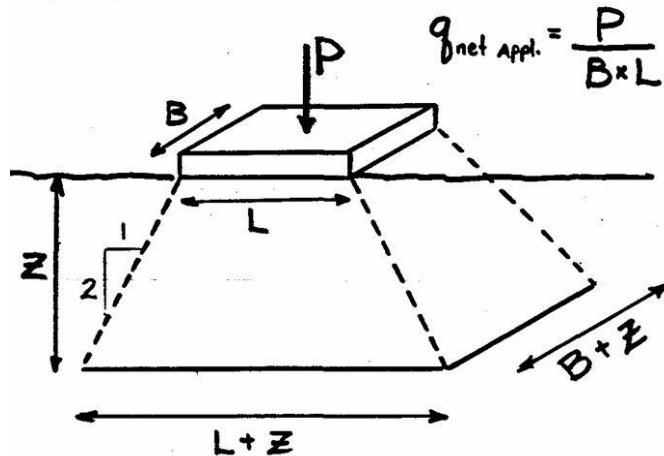


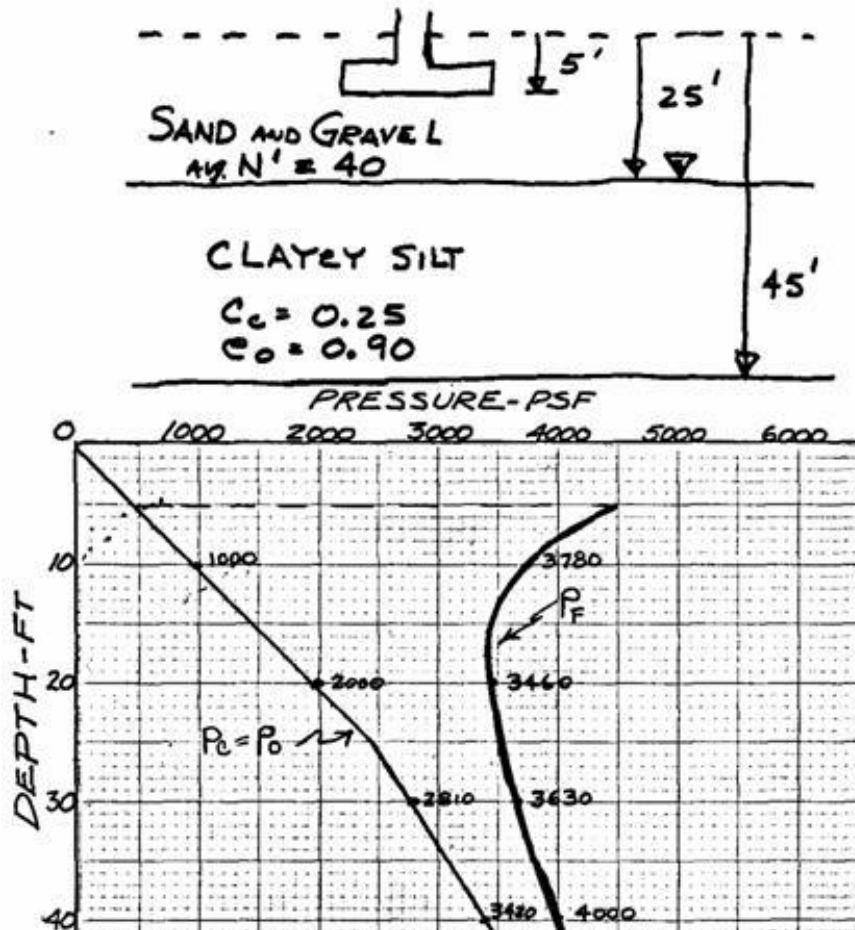
Figure 7: Definition of variables for stress increase via 2:1 rule.

Table 1: Typical secant modulus for geomaterials

Soil	Poisson's Ratio	E kg/cm ²
Clay	0.4 – 0.5	
Very soft		3 - 30
Soft		20 - 40
Medium		45 - 90
Hard		70 - 200
Sandy		300 - 425
Sand	0.2 – 0.4	
Silty		50 - 200
Loose		100 - 250
Dense		500 - 1000
Sand and gravel		
Dense		800 - 2000
Loose		500 - 1400
Silt	0.3 – 0.35	20 - 200

Sample Problem:

GIVEN SOIL PROFILE AND PRESSURE
DIAGRAM BELOW
FIND FOOTING SETTLEMENT USING
INCREMENTS OF 10'



Slope Stability

Introduction

It is not uncommon for the geotechnical engineer to encounter sloping ground, for example:

- Highway embankments and cuts
- Natural slopes

There are two factors to be considered:

- Stability - analysis usually based on limit equilibrium procedures
- Settlements – most important when, for example, dealing with bridge approaches where large differential settlements can present problems

Stability must be assured prior to consideration of other foundation related items. Within the context of embankments, problems usually occur when embankments are built over soft, weak soil layers.

Driving Forces for Instability:

- Increase in load at top of slope
- Change in slope
- Depth of cut/height of embankment
- Change in water table
- Earthquake/blast loading
- Time-dependent soil properties.

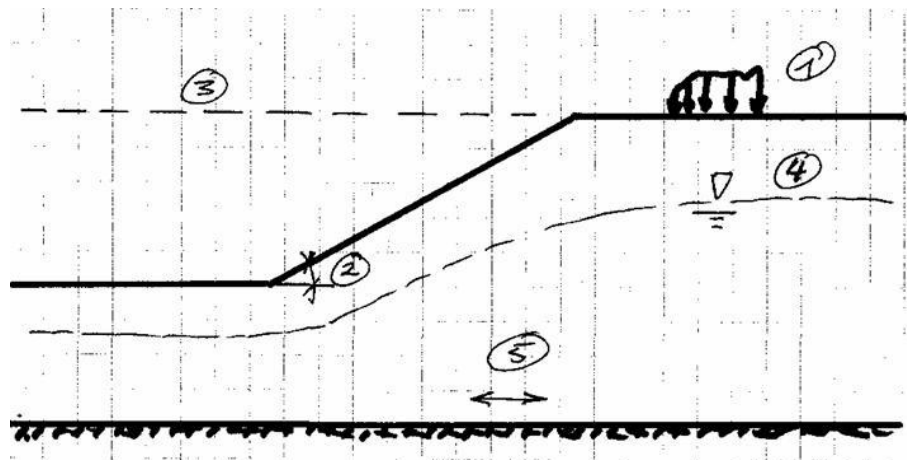


Figure 1: Changes leading to slope instability.

Effects of Water

- Decreases intergranular stresses (effective) due to buoyancy
- Introduces seepage forces
- Increases driving force due to extra weight
- For cohesive soils

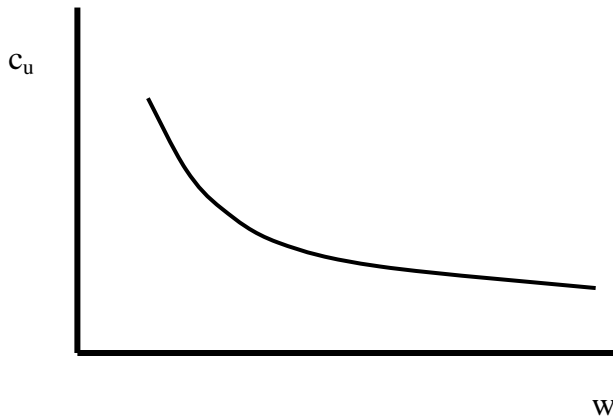


Figure 2: Relation between undrained shear strength and water content

- Slaking – sudden increase in moisture leading to sudden disintegration

Design Factor of Safety

By definition, we have

$$F_s = \frac{\tau_{available}}{\tau_{mobilized}}$$

For highway embankments,

$$F_s \geq 1.25 \text{ for normal situations}$$

$$F_s \geq 1.3 \text{ for critical situation}$$

The selection of the appropriate factor of safety depends on the analysis performed, reliability of data and consequences of failure.

Factor of Safety in Fine-Grained Soils

Embankments

Consider the embankment shown in Figure 3 and the corresponding potential failure surface. As the embankment is constructed, the average shear stress increases along the failure surface. As the stress state at P changes the invariants s and t also change, which according to Skempton's pore-water equation, yields

$$\Delta u_w = \Delta s + 2\left(A - \frac{1}{2}\right)\Delta t$$

For a normally consolidated soil, A is approximately 1. As the level of pre-consolidation in the foundation soil increases A decreases and can even become negative for heavily over-consolidated soils. In all practical cases however the resulting pore pressure increment will be positive.

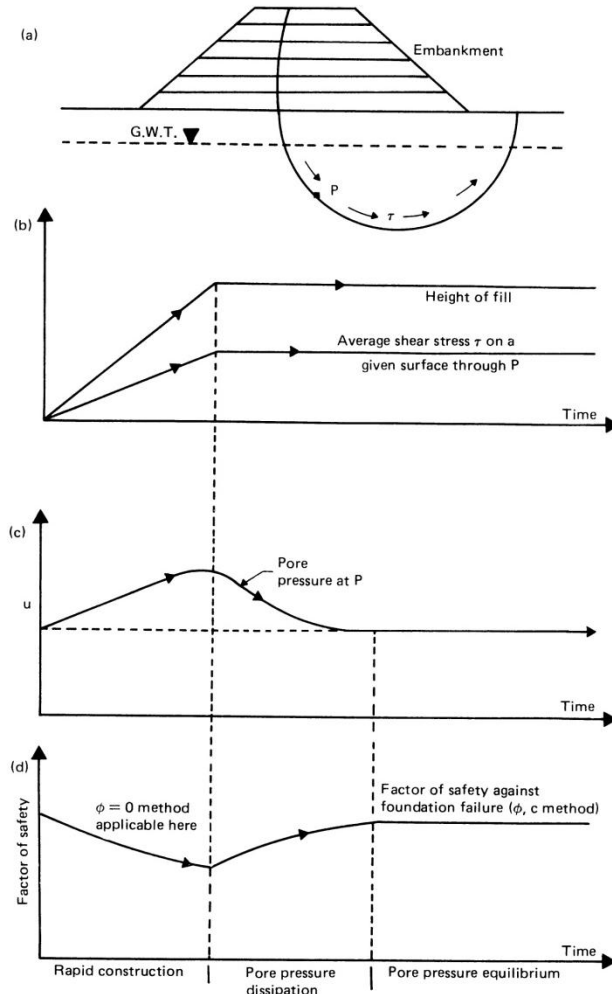


Figure 3. Foundation conditions beneath a fill.



Figure 4: Small slope instability of fill area.

Stability Analysis

Stability requires ensuring force and moment equilibrium; i.e.,

$$\sum \vec{F} = 0 \quad \text{and} \quad \sum \vec{r} \times \vec{F} = 0.$$

Unless the engineer makes use of, for example, the finite element method, analyses involve careful consideration of the potential failure modes and limit equilibrium conditions. Three failure modes are considered here, for illustration purposes; i.e., infinite slope, sliding block and slip circle.

Infinite Slope Failure

This failure mode usually does not present problems, but does highlight important design considerations. Referring to Figure 5, we consider a very long slope, which has the potential to fail along a plane that is parallel to the upper surface. If we consider the equilibrium of a typical block, one finds that the forces along the two sides are equal and opposite, thus canceling one another out. This means that the weight \vec{W} of the block must be balanced entirely by the forces \vec{N} and \vec{T} along the bottom. To simplify the exposition, the only case of no groundwater is presented.

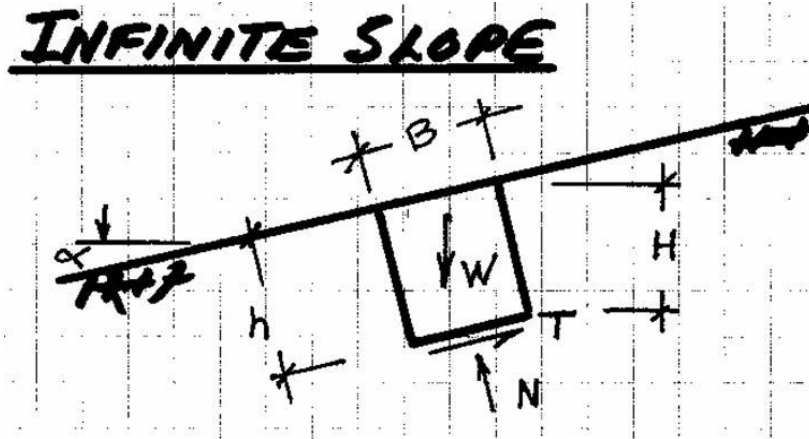


Figure 5: Schematic of infinite slope.

Assuming that the block has a unit width $B = 1$, equilibrium requires

$$N = \sigma_m = \gamma h \cos \alpha$$

$$T = \tau_m = \gamma h \sin \alpha$$

where the subscript m refers to the mobilized stresses. Given that $F_s = \tau_f / \tau_m$,

$$F_s = \frac{c + \gamma h \cos \alpha \tan \phi}{\gamma h \sin \alpha}$$

where failure depends on the Coulomb criterion. After rearranging terms and introducing depth/height H ,

$$F_s = \frac{N_f + \cos^2 \alpha \tan \phi}{\cos \alpha \sin \alpha}$$

with

$$N_f = \frac{c}{\gamma H}.$$

One observes:

- F_s is independent of H for a cohesionless soil.
- A slope of a cohesive soil can be stable if $\tan \alpha > \tan \phi'$

The following conditions are noteworthy for a cohesionless soil:

- Unsaturated or submerged slope - $F_s = \frac{\tan \phi'}{\tan \alpha}$
- Saturated with seepage parallel to slope - $F_s = \frac{\gamma' \tan \phi'}{\gamma \tan \alpha}$

Sliding Block Failure

Referring to Figure 6, if an embankment is built on a foundation, which contains a thin weak layer at shallow depths, any failure will most likely pass along this layer.

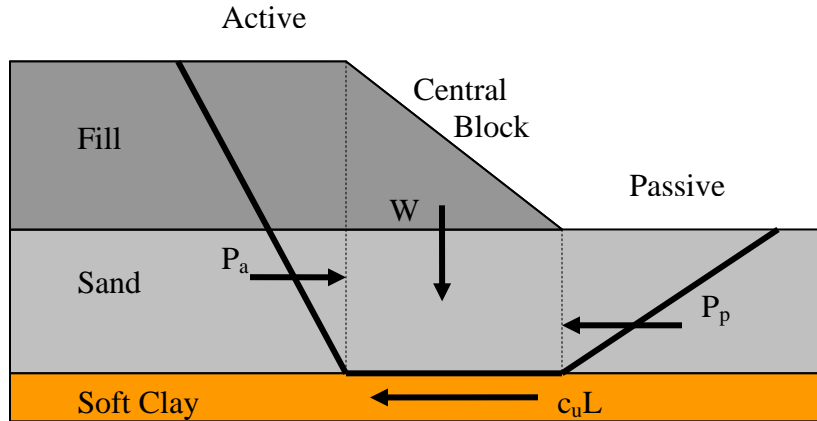


Figure 6: Main components of sliding block failure.

Given the definition of factor of safety,

$$F_s = \frac{\text{Horizontal Resisting Forces}}{\text{Horizontal Driving Forces}}$$

we may write assuming that the active and passive forces are given by Rankine theory,

$$F_s = \frac{P_p + c_u L}{P_a}$$

where the symbols take on their usual meanings, with L being the width of central block.

Slip Circle Analysis – Method of Slices

For many natural uniform slopes, the failure pattern appears to follow a circular arc. This has led to the well-known slip circle analysis, in which the focus is on the factor of safety with respect to moment equilibrium. Strictly speaking, one should consider both local and global force and moment equilibrium. Depending on the assumptions regarding the interslice forces X and Y, various definitions for F_s have been developed.

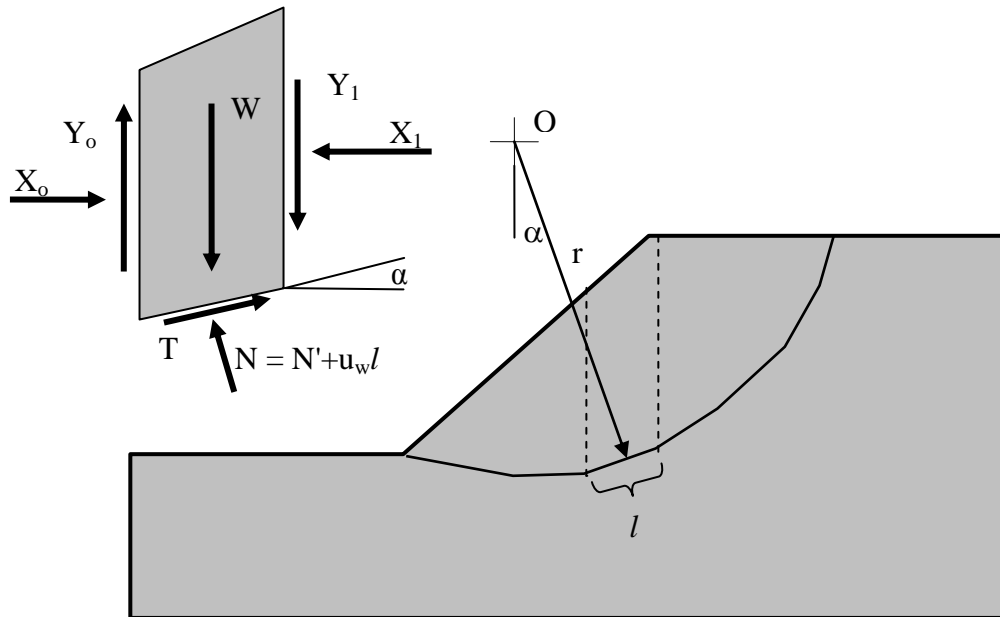


Figure 7: Main components for slip circle analysis.

Let us consider the slope shown in Figure 7. The usual procedure for stability analysis is to subdivide the slope contained within an assumed failure zone in number of slices (only one being shown). When taking into account all slices, moment equilibrium about O yields:

$$\sum Tr = \sum Wr \sin \alpha$$

Recall that for a circular arc, the normal forces N do not contribute to equilibrium.

For each slice we have a situation where for local equilibrium the mobilized shear is less than that corresponding to failure; i.e.,

$$T = \tau_m l \leq \tau_f l \quad \Rightarrow \quad \sum \tau_m lr = \sum Wr \sin \alpha \leq \sum \tau_f lr$$

We can now proceed to define the factor of safety

$$F_s = \frac{\sum \tau_f l}{\sum W \sin \alpha} \geq 1$$

for equilibrium.

Assuming effective stress analysis,

$$F_s = \frac{\sum (c' + \sigma'' \tan \phi') l}{\sum W \sin \alpha}$$

or

$$F_s = \frac{\sum (c' l + N' \tan \phi')}{\sum W \sin \alpha}$$

At this point it is important to recognize that we have not attempted to satisfy $\sum \vec{F} = 0$, on global and local levels. When force equilibrium is taken into account, this is usually done on the slice level.

Fellinius Solution

For the Fellinius approach, the effect of the interslice forces is ignored; i.e., $\Delta X \sim 0$ and $\Delta Y \sim 0$. Therefore,

$$N' = W \cos \alpha - u_w l \quad \Rightarrow \quad F_s = \frac{\sum (c' l + (W \cos \alpha - u_w l) \tan \phi')}{\sum W \sin \alpha}$$

This procedure usually underestimates the factor of safety by 5 to 20%. It tends to be overly conservative.

Modified Bishop's Simplified Method ($Y_1 - Y_o = 0$)

A slightly different approach is taken than is usually presented in textbooks. We begin by taking proper account of vertical equilibrium of a slice,

$$W = N \cos \alpha + T_m \sin \alpha + \Delta Y .$$

Recognizing that $T_m = \tau_m l \leq T_f = \tau_f l$, we can write

$$W \leq N \cos \alpha + T_f \sin \alpha + \Delta Y$$

or

$$W \leq (N' + u_w l) \cos \alpha + (c' l + N' \tan \phi') \sin \alpha + \Delta Y.$$

Rearranging this equation yields,

$$N' \geq \frac{W - u_w l \cos \alpha - c' l \sin \alpha - \Delta Y}{\cos \alpha + \tan \phi' \sin \alpha}$$

or by recognizing that we are conservative by neglecting the inequality we have

$$N' = \frac{(W \cos \alpha - u_w l) + u_w l \sin^2 \alpha - c' l \sin \alpha \cos \alpha - \Delta Y}{\cos^2 \alpha (1 + \tan \phi' \tan \alpha)}.$$

After substituting for N'

$$F_s = \frac{\sum \left(c' l + \left[\frac{W - u_w l \cos \alpha - c' l \sin \alpha - \Delta Y}{\cos \alpha + \tan \phi' \sin \alpha} \right] \tan \phi' \right)}{\sum W \sin \alpha}$$

Assuming that $\sum \frac{\Delta Y \tan \phi'}{\cos \alpha + \tan \phi' \sin \alpha}$

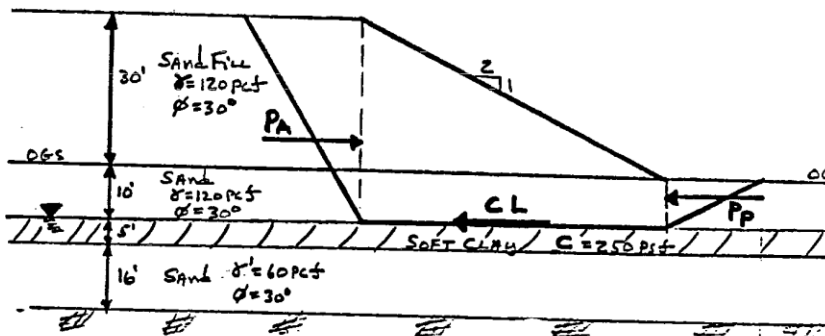
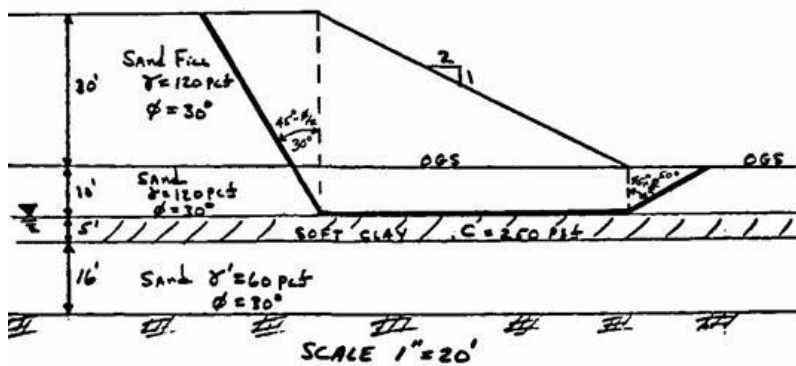
$$F_s = \frac{\sum \left(c' l + \left[\frac{W - u_w l \cos \alpha - c' l \sin \alpha}{\cos \alpha + \tan \phi' \sin \alpha} \right] \tan \phi' \right)}{\sum W \sin \alpha}$$

When using this equation for N' , the factor of safety is usually underestimated by 2% when compared to the so-called more accurate procedures. However, if the exist angle exceeds 30%, the procedure may overestimate the factor of safety.

Note: Here we have only considered one potential failure surface. In actual fact, it is necessary to repeat this calculation to identify the surface with the lowest factor of safety.

Sample Problem 1:

(I) USING A SLIDING BLOCK ANALYSIS,
DETERMINE THE SAFETY FACTOR
AGAINST SLIDING FOR THE EMBANKMENT
AND ASSUMED FAILURE SURFACE SHOWN.



$$(I) K_A = \tan^2(45^\circ - \frac{\phi}{2}) = \tan^2(45^\circ - 30^\circ/2) = 0.33$$

$$K_P = \tan^2(45^\circ + \frac{\phi}{2}) = \tan^2(45^\circ + 30^\circ/2) = 3.0$$

$$(\text{PER FT}) P_A = \frac{1}{2} \gamma H^2 K_A = \frac{1}{2} (120 \text{ kcf})(40 \text{ ft})^2 (0.33)(1 \text{ ft}) = 32 \text{ k} \rightarrow$$

$$P_P = \frac{1}{2} \gamma H^2 K_P = \frac{1}{2} (120 \text{ kcf})(10 \text{ ft})^2 (3.0)(1 \text{ ft}) = 18 \text{ k} \leftarrow$$

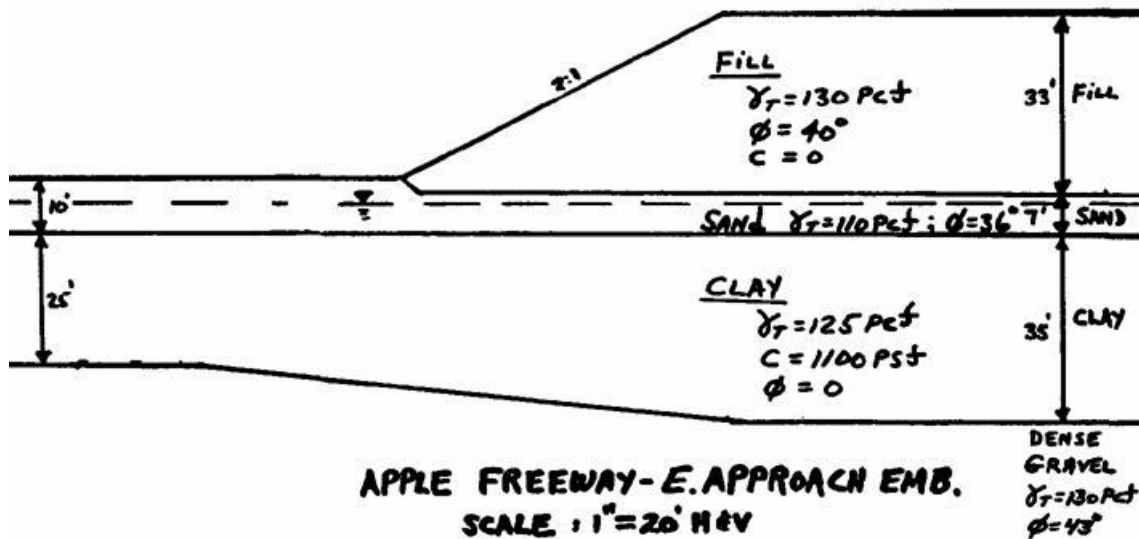
$$CL = (0.250 \text{ ksf})(60 \text{ ft})(1 \text{ ft}) = 15 \text{ k} \leftarrow$$

SUMMING FORCES HORIZONTALLY:

$$F.S. = \frac{\sum \text{RESISTING FORCES}}{\sum \text{DRIVING FORCES}} = \frac{P_P + CL}{P_A} = \frac{18 \text{ k} + 15 \text{ k}}{32 \text{ k}}$$

$\therefore F.S. = 1.03$ Too Low!! < 1.25

Sample Problem 2.

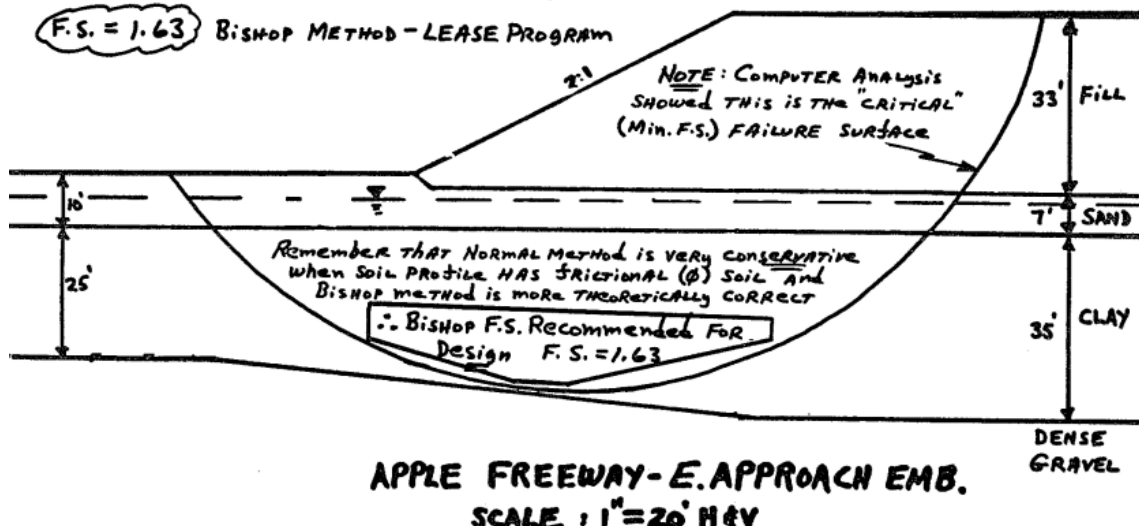


COMPARISON OF FACTORS OF SAFETY

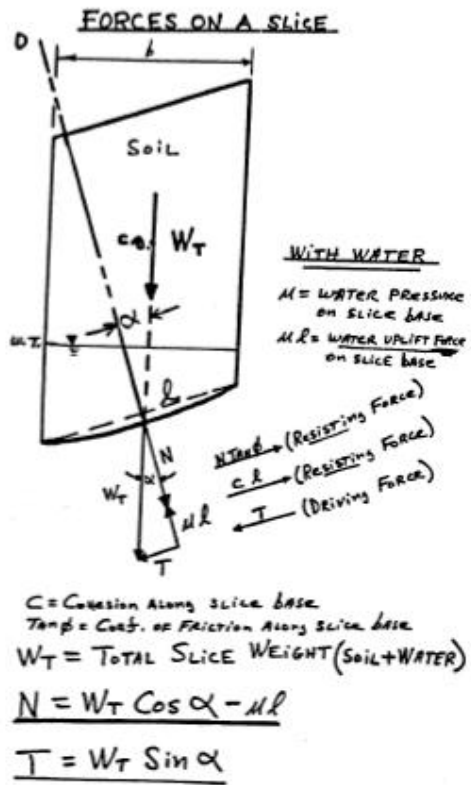
F.S. = 1.35 NORMAL METHOD - Hand Solution

F.S. = 1.37 NORMAL METHOD - LEASE PROGRAM

F.S. = 1.63 BISHOP METHOD - LEASE PROGRAM



Details:

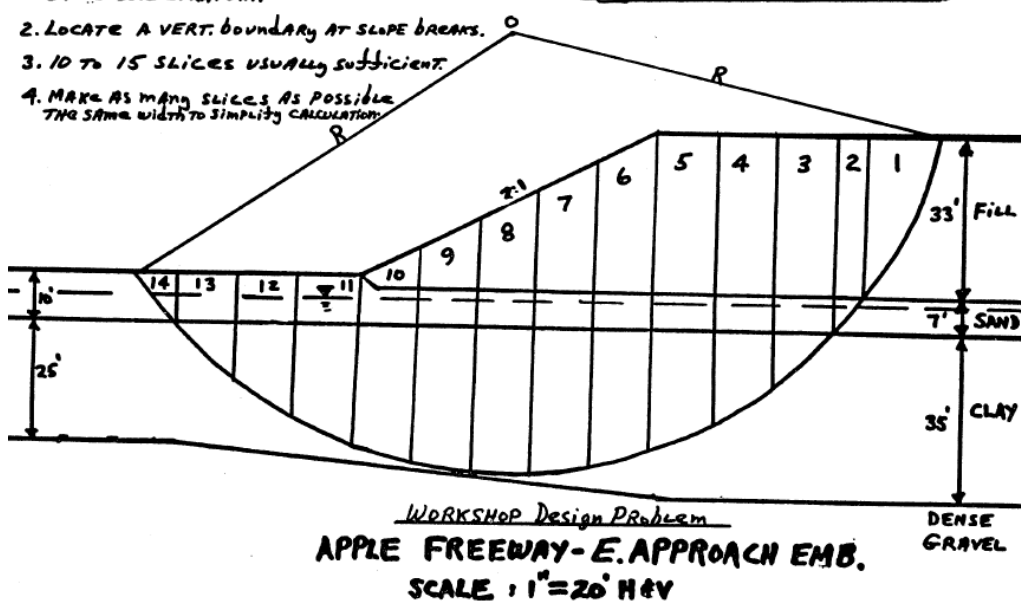


General Notes:

1. LOCATE VERT. boundary of Slice so THAT Slice base is entirely in THE SAME SOIL STRATUM.
2. LOCATE A VERT. boundary AT SLOPE BREAKS.
3. 10 TO 15 SLICES USUALLY SUFFICIENT.
4. MAKE AS MANY SLICES AS POSSIBLE THE SAME WIDTH TO SIMPLIFY CALCULATIONS.

(CIRCULAR ARC ANALYSIS cont'd)

Divide Mass Above Failure Surface INTO VERTICAL SLICES



GENERAL NOTES (CONT'D)

5. DRAW LINE FROM CIRCLE CENTER O
TO SLICE BASE FOR ALL SLICES.

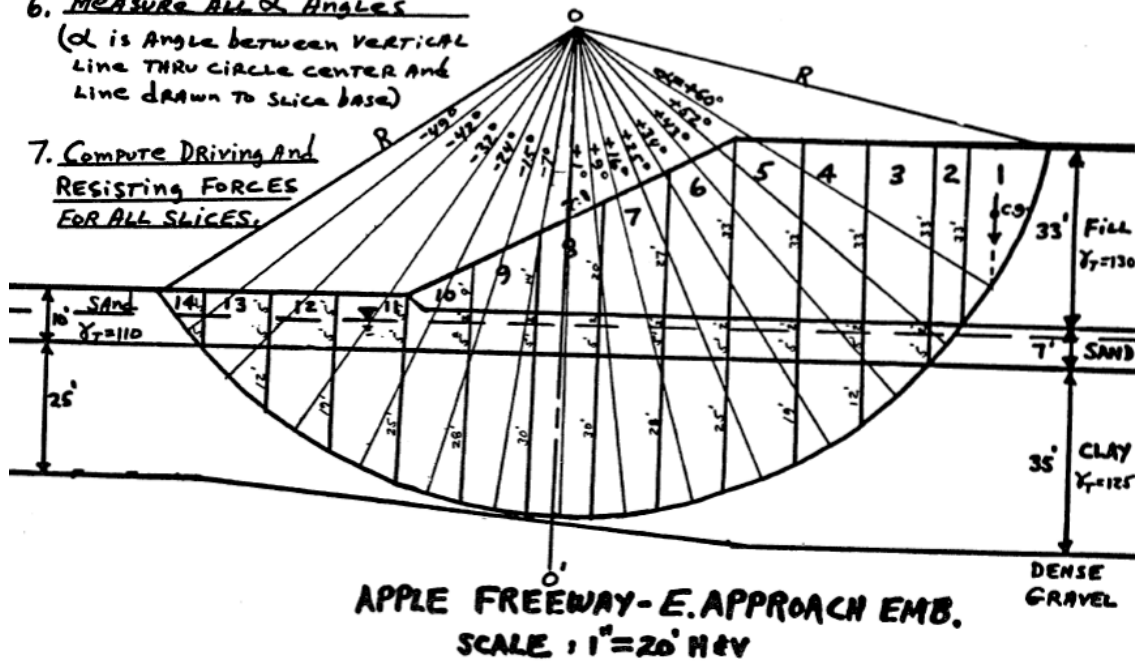
6. MEASURE ALL α ANGLES

(α is Angle between VERTICAL
Line THRU CIRCLE CENTER AND
Line drawn to Slice base)

7. Compute Driving And
RESISTING FORCES
FOR ALL SLICES.

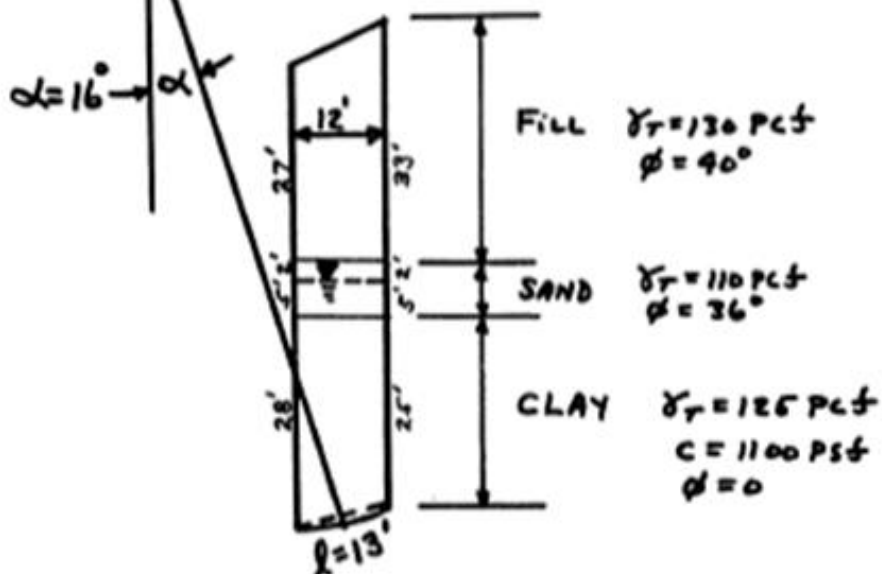
CIRCULAR ARC ANALYSIS (cont'd)

WORKSHOP Design Problem



EXAMPLE COMPUTATION

APPLE Freeway Problem - SLICE 6



$$W_T = (12) \left(\frac{27+33}{2} \right) (130) + (12)(7)(110) + (12) \left(\frac{28+25}{2} \right) (125) = 95,790 \text{ lb}$$

$$\alpha = +16^\circ$$

$$T = W_T \sin \alpha = 95,790 \text{ lb} (\sin 16^\circ) = 26,403 \text{ lb}$$

BOTTOM OF SLICE IS IN CLAY WHERE $\phi = 0$
 $\therefore N \tan \phi = 0$

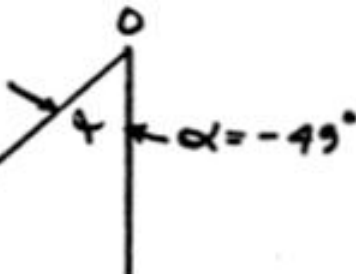
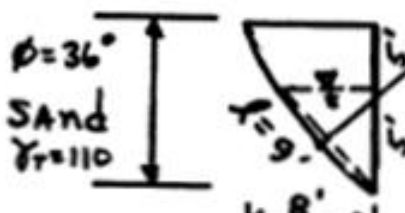
$$C \ell = (1100)(13) = 14,300 \text{ lb}$$

\therefore FOR SLICE 6: $\leftarrow T = 26,403 \text{ lb}$ (Driving Force)
 $\rightarrow C \ell = 14,300 \text{ lb}$ (Resisting Force)

$N \tan \phi = 0$ since $\phi = 0$

EXAMPLE Computation

SLICE 14



$$W_T = (8)(14\text{ ft})(110) = 9,400 \text{ lb}$$

$$-T = W_T \sin \alpha = 9,400 \text{ lb} (\sin -49^\circ) = -3,321 \text{ lb}$$

NOTE: T is a minus for this slice
since it tends to RESIST SLIDING

BOTTOM OF SLICE IS IN SAND WITH $\phi = 36^\circ$
 $C = 0$
 $\therefore C_l = 0$

$$N = W_T \cos \alpha - M l = (9,400 \text{ lb}) (\cos 49^\circ) - (5/2)(60)(9)$$

$$= 2,887 - 1350 = 1537 \text{ lb}$$

$$N \tan \phi = 1537 \text{ lb} (\tan 36^\circ) = 1117 \text{ lb}$$

∴ FOR SLICE 14:

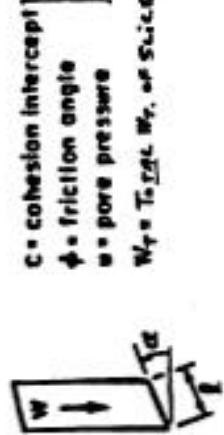
$$\rightarrow T = -3,321 \text{ lb (Driving Force)}$$

$$\rightarrow N \tan \phi = 1117 \text{ lb (Resisting Force)}$$

$$C_l = 0 \quad \text{Since } C = 0$$

Workshop Design Problem
Circular Arc Analysis (cont'd)

Slice No.	w_r	θ	I	α	c	ϕ	σ	u_f	w_{psat}	$\frac{w_{psat} - w_r}{2}$	cI	$T = \frac{w_r}{w_{psat}}$
(A)	(fr)	(Lgnd)	(est)	(Lgnd)	(est)	(fr)	(Lgnd)	(fr)	(Lgnd)	(fr)	(fr)	(fr)
1	32,775	36	60	0	40	0	0	0	16,025	15,399	0	27.814
2	28,450	10	52	0	36	450	5500	17,269	15,769	11,457	0	22.031
3	62,720	17	43	1100	0	660	7,920	—	—	0	0	18,700
4	83,975	15	34	1100	0	1,230	18,450	—	—	0	0	16,500
5	93,720	15	25	1100	0	1,620	24,300	—	—	0	0	16,500
6	95,750	13	16	1100	0	1,890	24,520	—	—	0	0	16,455
7	89,400	13	9	1100	0	2,090	26,520	—	—	0	0	16,300
8	80,710	12	1	1100	0	2,100	25,200	—	—	0	0	13,300
9	70,480	12	-7	1100	0	2,040	24,480	—	—	0	0	13,200
10	49,310	13	-15	1100	0	1,890	24,520	—	—	0	0	14,300
11	59,050	14	-24	1100	0	1,620	22,680	—	—	0	0	15,400
12	36,410	14	-32	1100	0	1,230	17,220	—	—	0	0	15,400
13	22,260	16	-42	1100	0	660	10,560	—	—	0	0	17,600
14	4,400	9	-45	0	36	1,510	1,360	2,887	1,537	1117	0	-3,321
												1 26,073 / 69,400 / 44.311



c = cohesion intercept
 ϕ = friction angle
 w = pore pressure
 $w_r = T_c \tan \phi + S_c \sin \phi$

$$w_r = \frac{26,073 + 169,400}{148,311} = 1.35$$

$$F = \frac{T_c \tan \phi + S_c \sin \phi}{w_{psat}} = \frac{\Sigma N T_c \tan \phi + \Sigma S_c \sin \phi}{\Sigma T_c}$$

TABULAR FORM FOR CALCULATING FACTOR OF SAFETY BY ORDINARY METHOD OF SLICES.